# 99mTc-Cyclopentadienyl Tricarbonyl Chelate-Labeled Compounds as Selective Sigma-2 Receptor Ligands for Tumor Imaging

Li, D.; Chen, Y.; Wang, X.; Deuther-Conrad, W.; Chen, X.; Jia, B.; Dong, C.; Steinbach, J.; Brust, P.; Liu, B.; Jia, H.;

Originally published:

January 2016

**Journal of Medicinal Chemistry 59(2016)3, 934-946**

DOI: https://doi.org/10.1021/acs.jmedchem.5b01378

# $^{99m}$Tc-cyclopentadienyl Tricarbonyl Chelate-labeled Compounds as Selective Sigma-2 Receptor Ligands for Tumor Imaging

Dan Li[†II], Yuanyuan Chen[†II], Xia Wang[†], Winnie Deuther-Conrad[‡], Xin Chen[†], Bing Jia[§], Chengyan Dong[¶], Jörg Steinbach[‡], Peter Brust[‡], Boli Liu[†], Hongmei Jia[†*]

[†]Key Laboratory of Radiopharmaceuticals (Beijing Normal University), Ministry of Education, College of Chemistry, Beijing Normal University, Beijing 100875, China;
[‡]Helmholtz-Zentrum Dresden-Rossendorf, Institute of Radiopharmaceutical Cancer Research/ Department of Neuroradiopharmaceuticals, 04318 Leipzig, Germany
[§]Medical and Healthy Analytical Center, Peking University, Beijing 100191, China
[¶] Interdisciplinary Laboratory, Institute of Biophysics, Chinese Academy of Sciences, Beijing 100101, China

Corresponding author:
*To whom correspondence should be addressed: Phone: +86-10-58808891; Fax: +86-10-58808891. Email: hmjia@bnu.edu.cn

Author Contributions：
[II]Both authors contributed equally to this work.

## Abstract

We have designed and synthesized a series of cyclopentadienyl tricarbonyl rhenium complexes containing 5,6-dimethoxyisoindoline or 6,7-dimethoxy-1,2,3,4-tetrahydroisoquinoline pharmacophore as $\sigma_2$ receptor ligands. Rhenium compound **20a** possessed low nanomolar $\sigma_2$ receptor affinity ($K_i$ = 2.97 nM) and moderate subtype selectivity (10-fold). Moreover, it showed high selectivity towards vesicular acetylcholine transporter (2374-fold), dopamine $D_{2L}$ receptor, NMDA receptor, opiate receptor, dopamine transporter, norepinephrine transporter, and serotonin transporter. Its corresponding radiotracer [$^{99m}$Tc]**20b** showed high uptake in a time- and dose-dependent manner in DU145 prostate cells and C6 glioma cells. In addition, this tracer exhibited high tumor uptake (5.92 %ID/g at 240 min) and high tumor/blood and tumor/muscle ratios (21 and 16 at 240 min, respectively) as well as specific binding to σ receptors in nude mice bearing C6 glioma xenografts. Small animal SPECT/CT imaging of [$^{99m}$Tc]**20b** in the C6 glioma xenograft model demonstrated a clear visualization of the tumor at 180 min postinjection.


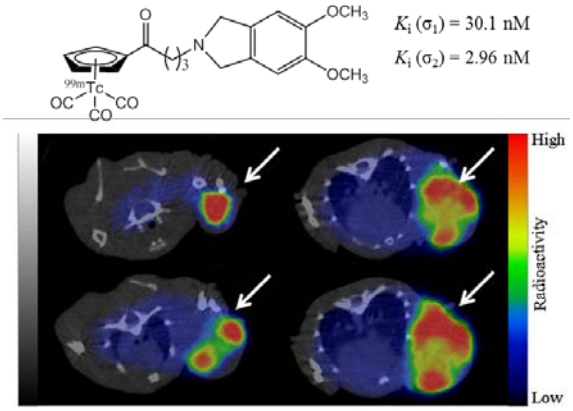

## INTRODUCTION

Uncontrolled cell proliferation is one of the hallmarks of cancer and its assessment will provide useful information to predict the tumor aggressiveness and prognosis of cancer.[1] The sigma-2 ($\sigma_2$) receptors are upregulated in a wide variety of human and rodent tumor cells.[2-6] Moreover, they showed an approximately 10-fold higher expression in proliferating versus quiescent tumors.[7-9] Significant effort has been dedicated to the validation of the $\sigma_2$ receptor as a biomarker for imaging of proliferative status of solid tumors.[7-15] Currently, a promising radiotracer targeting $\sigma_2$ receptors, *N*-(4-(6,7-dimethoxy-3,4-dihydroisoquinolin-2(1*H*)-yl)butyl)-2-(2-[$^{18}$F]fluoroethoxy)-5-methylbenzamide ([$^{18}$F]ISO-1) is under clinical trials.[10-12] Furthermore, a significant correlation between uptake of this radiotracer and Ki-67 (the "gold standard" used in histological measurements of cell proliferation in tumor surgical and biopsy specimens) was observed in human studies.[12] These findings indicate that the $\sigma_2$ receptor is an important biomarker for determining the proliferative status of solid tumors using positron emission tomography (PET).[13-15]

It is well known that single photon emission computed tomography (SPECT) is an extremely helpful, widely used and low cost clinical imaging modality. $^{99m}$Tc is still the most widely used radionuclide in clinical nuclear medicine application. With the clinical implementation of quantitative SPECT in the future,[16] $^{99m}$Tc-labeled radiotracers with high affinity, high selectivity and specificity for $\sigma_2$ receptors will provide a unique tool for the early diagnosis of cancer and assessment of the proliferative status of solid tumors. Over the past few decades, a series of $^{99m}$Tc-labeled radioligands targeting $\sigma_2$ receptors have been reported.[17-22] However, there is a lack of ideal $^{99m}$Tc-labeled radiotracers for imaging $\sigma_2$ receptors in human studies. Therefore, development of $^{99m}$Tc-labeled $\sigma_2$ receptor radioligands is very attractive.

Previously, our structure-affinity relationship analyses indicated the high importance of the $\sigma_2$ preferring group to improve the selectivity for $\sigma_2$ receptors.[23] Besides the 6,7-dimethoxy-1,2,3,4-tetrahydroisoquinoline scaffold in ISO-1, the 5,6-dimethoxyisoindoline moiety was identified as a promising $\sigma_2$ preferring group with less lipophilicity.[24] Moreover, the [(Cp-R)Tc(CO)$_3$] unit can be incorporated into selective receptor ligands without a significant change in the biological properties via an appropriate linker.[22, 25] In the present study, our aim is to develop a $^{99m}$Tc-labeled radioligand as a selective $\sigma_2$ receptor probe for tumor imaging with SPECT. The design concept is shown in Figure 1.

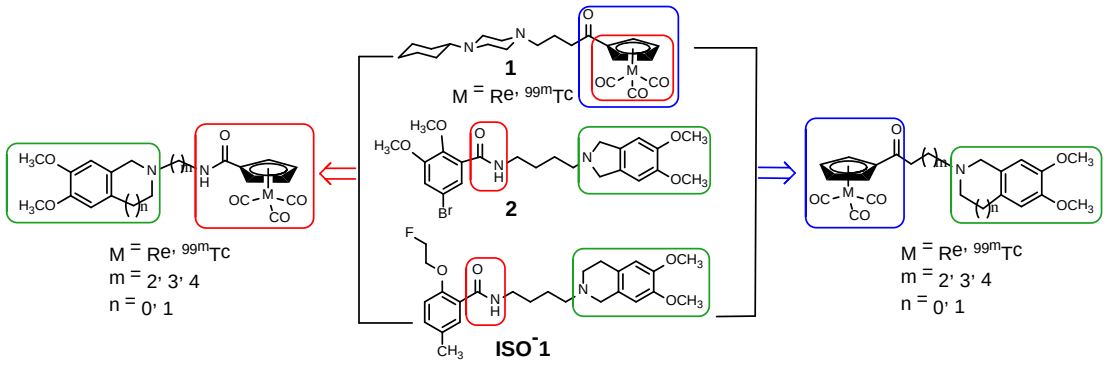


**Figure 1**. Design concept of novel [(Cp-R)M(CO)$_3$] (M = $^{99m}$Tc, Re) complexes as potent $\sigma_2$ receptor ligands.

**Scheme 1**. Synthetic routes of the rhenium compounds

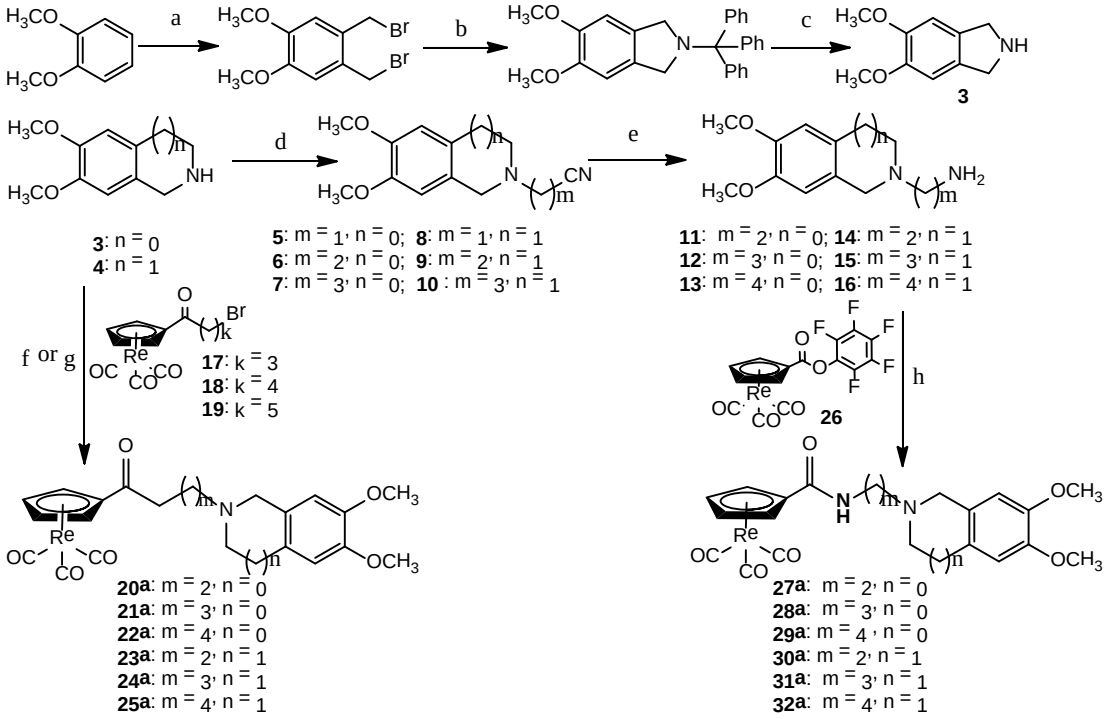

Reagents and conditions: (a) 33% HBr/HOAc, rt (20 h) – 65 °C (1 h), 32%; (b) tritylamine, DIEA, DMF, 60 °C, 2 h, 77%; (c) TFA, $CHCl_3$/MeOH, 0 °C – rt, 1 h, 69%; (d) $Br(CH_2)_mCN$, $Et_3N$, $CH_2Cl_2$, rt, 24 h, for **5**–**7**, 67–73%, for **8**–**10**, 59–70%; (e) $LiAlH_4$, THF-$Et_2O$, 0 °C – rt, 24 h, for **11**–**13**, 36–50%, for **14**–**16**, 27–40%; (f) toluene, **3** or **4**, KI, $Et_3N$, 115 °C, 10% for **20a**, 10% for **21a**, 30% for **23a** and 36% for **24a**; (g) acetonitrile, **3** or **4**, KI, $K_2CO_3$, 90 °C, 41% for **22a** and 51% for **25a**; (h)**11**–**16**, $Et_3N$, anhydrous DMF, rt, 4 h, 38–48% for **27a**–**29a**, 74–83% for **30a**–**32a**.

In the first approach, we directly incorporate the [(Cp-R)Tc(CO)$_3$] unit containing carbonyl group in compound **1** with the $\sigma_2$ preferring group (5,6-dimethoxyisoindoline moiety in compound **2** or 6,7-dimethoxy-1,2,3,4-tetrahydroisoquinoline moiety in ISO-1) via different carbon chain lengths. In the second approach, the amide group was connected to the [(Cp-R)M(CO)$_3$] (M = Re, $^{99m}$Tc) unit in compound **1** first, and then incorporated with a $\sigma_2$ preferring group. Both carbonyl and amide groups are electron-withdrawing groups and would allow the double ligand transfer (DLT) reaction for the efficient synthesis of the $^{99m}$Tc-complex from the corresponding ferrocene precursor. In addition, different carbon chain lengths were used as the linker between the [(Cp-R)M(CO)$_3$] unit with an electron-withdrawing group and the 5,6-dimethoxyisoindoline or 6,7-dimethoxy-1,2,3,4-tetrahydroisoquinoline pharmacophore to find the optimal radiotracer with appropriate interaction on $\sigma_2$ receptors for *in vivo* tumor imaging. Herein, we report the syntheses of novel [(Cp-R)M(CO)$_3$] (M = Re, $^{99m}$Tc) complexes containing 5,6-dimethoxyisoindoline or 6,7-dimethoxy-1,2,3,4-tetrahydroisoquinoline motif, and we evaluated them as potential $\sigma_2$ receptor radioligands for tumor imaging *in vivo*.

## RESULTS

### Chemistry

For the characterization of $^{99m}$Tc-labeled compounds, the surrogates of the corresponding rhenium complexes were prepared and the synthetic routes are depicted in Scheme 1. Intermediates **3**,[26] **8**–**10**,[27] **14**–**16**,[27] **17**–**19**[22] and **26**[28] were obtained according to the methods reported in the literature. *N*-Alkylation of compound **3** or **4** with compounds **17**–**19** gave compounds **20a**–**25a** (**20a**, **22a**, **23a** and **25a**)[29], respectively, with yields of 10–51%. It needs to be mentioned that compounds **22a** and **25a** could be obtained with higher yields in acetonitrile with $K_2CO_3$ as base than in toluene with triethylamine. On the other hand, *N*-alkylation of compound **3** with bromine-substituted nitrile, followed by reduction with $LiAlH_4$ provided compounds **11**–**13**, respectively, with yields of 36–50%. The activated ester **26** reacted with the corresponding amine analogues **11**–**16** in anhydrous DMF at room temperature to afford the target rhenium analogues **27a**–**32a** (**27a**, **28a** and **29a**)[30]. Complex **31a** could be re-crystallized by slow evaporation of a mixture of methylene dichloride and hexane solution to afford X-ray diffraction crystals.

To further confirm the chemical structure and examine the binding model of $^{99m}$Tc-labeled cyclopentadienyl tricarbonyl complexes, the single X-ray crystal structure analysis of complex **31a** was performed. Crystal structure data together with details of the determinations are summarized in the Supporting Information (Tables S1–5). The crystal structure with the atomic numbering scheme of compound **31a** is shown in Figure 2.

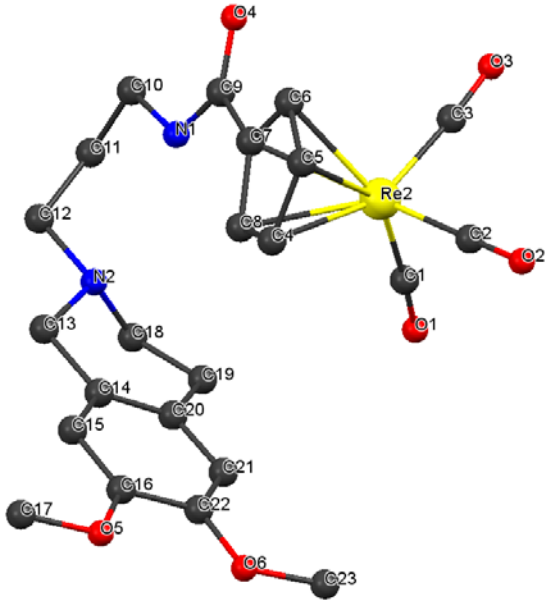


**Figure 2**. Crystal structure of compound **31a**.

The central rhenium atom is $\eta^5$-coordinated to the cyclopentadienyl ring, and the coordination sphere is completed by three carbonyl groups. The average bond lengths of Re–C (Cp) and Re–C (CO) are 2.30 and 1.91 Å, respectively. The bond angle of C–Re–C (between CO) is approximately 90°. The distance between the *N*-atom and the center of the aromatic ring of 6,7-dimethoxy-1,2,3,4-tetrahydroisoquinoline residue is 3.70 Å. The distance between the *N*-atom and the center of the Cp ring of the [$CpM(CO)_3$] core is 5.05 Å.

***In vitro* radioligand competition studies**

The radioligand competition experiments were conducted as previously reported.[20] Typically, (+)-[$^3$H]pentazocine was used for the $\sigma_1$ receptors and [$^3$H]-1,3-di-*o*-tolyl-guanidine ([$^3$H]DTG) in the presence of 10 μM dextrallorphan were used for the $\sigma_2$ receptors. The affinities of the rhenium complexes and ferrocene precursors for $\sigma_1$ and $\sigma_2$ receptors are listed in Table 1. In general, the carbon length of the linker displayed significant influence on the affinity and subtype selectivity. Rhenium complexes with a carbonyl group displayed higher affinities for $\sigma_2$ receptors than those with an amide group (**20a**–**25a** *vs*. **27a**–**32a**). Compound **20a** and **24a** possessed nanomolar affinity for $\sigma_2$ receptors and moderate subtype selectivity. Compounds **23a,**[29] **29a**[30] and **30a** displayed comparable affinity for $\sigma_2$ receptors and subtype selectivity to ISO-1. Similar to our previous findings, ferrocene precursors with a carbonyl group displayed comparable affinity for $\sigma_2$ receptors to the corresponding rhenium complexes (**36** *vs*. **20a**, **38** *vs*. **22a**, **39** *vs*. **23a**, **41** *vs*. **25a**) and a little higher subtype selectivity.

**Table 1**. Binding affinities of cyclopentadienyl tricarbonyl rhenium complexes and ferrocene precursors for $\sigma_1$ and $\sigma_2$ receptors[a]

| Compound | $K_i$ ($\sigma_1$) (nM) | $K_i$ ($\sigma_2$) (nM) | $K_i(\sigma_1)/K_i(\sigma_2)$ |
|---|---|---|---|
| **20a** | 30.1 ± 11.3 | 2.96 ± 0.15 | 10.2 |
| **21a** | 6.67 ± 0.36 | 17.4 ± 2.2 | 0.4 |
| **22a** | 5.99 ± 1.72 | 10.2 ± 4.2 | 0.6 |
| **23a** | 121 ± 10 | 20.9 ± 0.2 | 5.8 |
| **24a** | 19.5 ± 4.2 | 7.42 ± 1.11 | 2.6 |
| **25a** | 6.46 ± 1.45 | 13.9 ± 7.5 | 0.5 |
| **27a** | 167 ± 49 | 508 ± 132 | 0.3 |
| **28a** | 524 ± 6 | 444 ± 242 | 1.2 |
| **29a** | 296 ± 104 | 22.6 ± 0.5 | 13.1 |
| **30a** | 309 ± 21 | 35.0 ± 10.1 | 8.8 |
| **31a** | 146 ± 65 | 41.0 ± 10.5 | 3.6 |
| **32a** | 187 ± 3 | 127 ± 48 | 1.5 |
| **36** | 137 ± 20 | 10.5 ± 0.7 | 13.0 |
| **38** | 19.2 ± 1.6 | 18.2 ± 3.3 | 1.1 |
| **39** | 240 ± 115 | 18.0 ± 1.4 | 13.3 |
| **41** | 13.3 ± 6.3 | 10.0 ± 0.3 | 1.3 |
| **43** | 98 ± 39 | 15.2 ± 0.1 | 6.5 |
| **44** | 1300 ± 305 | 60.2 ± 1.9 | 21.6 |
| **45** | 181 ± 25 | 30.0 ± 0.4 | 6.0 |
| **46** | 155 ± 27 | 23.5 ± 5.8 | 6.6 |
| **ISO-1**[b] | 330 ± 25 | 6.95 ± 1.63 | 47.5 |
| **ISO-1**[c] | 102 ± 15 | 28.2 ± 0.9 | 3.6 |
| **Siramesine**[c] | 4.69 ± 2.36 | 3.08 ± 0.68 | 1.5 |
| **Siramesine**[d] | 17 | 0.12 | 140 |
| **Siramesine**[e] | 10.5 ± 2.6 | 12.6 ± 0.1 | 0.8 |
| **Haloperidol**[f] | 4.95 ± 1.74 | 20.7 ± 0.07 | 0.2 |

[a] Values are means ± standard deviation (SD) of at least two experiments performed in triplicate.
[b] From ref 10.
[c] From ref 23.
[d] $IC_{50}$ value, from ref 31.
[e] From ref 32.
[f] From ref 33.

Considering the low nanomolar affinity and subtype selectivity of compound **20a** for $\sigma_2$ receptors, its affinities for the additional receptors and transporters were further tested. Compound **20a** exhibited very low affinity for VAChT ($K_i$(VAChT) = 7026 ± 163 nM) and was thus characterized by an excellent selectivity for $\sigma_2$ receptors ($K_i$(VAChT)/$K_i$($\sigma_2$) = 2374). Moreover, this ligand also displayed low affinity for dopamine $D_{2L}$ receptors, MNDA receptors, opiate receptors, dopamine transporter (DAT), norepinephrine transporter (NET), and serotonin transporter (SERT) as shown in Table S6 in the Supporting Information.

## Radiolabeling

Considering the moderate to high affinity and selectivity of the rhenium complexes **20a**–**25a** and **29a**–**30a** for $\sigma_2$ receptors, the corresponding $^{99m}$Tc-labeled radiotracers were prepared. The synthetic routes of the ferrocene precursors were similar to those of the corresponding rhenium compounds as shown in Scheme 2. The desired $^{99m}$Tc-labeled radiotracers were obtained via DLT reaction as shown in Scheme 3. After purification by semipreparative high performance liquid chromatography (HPLC), [$^{99m}$Tc]**20b**–**25b** ([$^{99m}$Tc]**20b**, [$^{99m}$Tc]**22b**, [$^{99m}$Tc]**23b** and [$^{99m}$Tc]**25b**)[29] and [$^{99m}$Tc]**29b**–**30b** ([$^{99m}$Tc]**29b**)[30] were obtained with radiochemical yields of 13–67% and a radiochemical purity of >99%.

**Scheme 2**. Synthetic routes for the ferrocene precursors

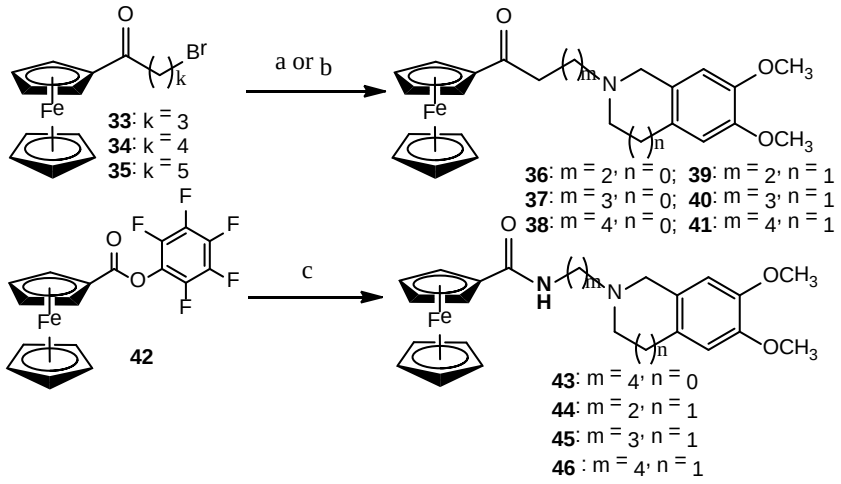


Reagents and conditions: (a) toluene, **3** or **4**, KI, $Et_3N$, 115 °C, 16% for **36**, 19% for **37**, 33% for **39** and 22% for **40**; (b) acetonitrile, **3** or **4**, KI, $K_2CO_3$, 90 °C, 44% for **38** and 78% for **41**; (c)**13**–**16**, $Et_3N$, anhydrous DMF, rt, 4 h, 65% for **43**, 69% for **44**, 63% for **45**, 68% for **46**.

## *In vitro* evaluation of the $^{99m}$Tc-labeled complexes

### Lipophilicity

For *in vitro* properties, the lipophilicity of the radiotracer is an important factor in the prediction of its free fraction in the plasma, the ability to across the blood-brain barrier (BBB) and nonspecific binding *in vivo*.[34,35] The measurement of the partition coefficients between 1-octanol and 0.05 M sodium phosphate buffer at pH = 7.4 was executed using a shake flask method.[22,36] The log *D* values of [$^{99m}$Tc]**20b**–**25b** and [$^{99m}$Tc]**29b**–**30b** were 2.56 ± 0.08,[29] 2.44 ± 0.02, 2.56 ± 0.08,[29] 2.61 ± 0.05, 2.92 ± 0.02, 2.60 ± 0.06, 2.39 ± 0.05[30] and 2.36 ± 0.01, respectively. The moderate lipophilicity of the above radiotracers may lead to decreased nonspecific binding and enhanced specific binding signal *in vivo*.

**Scheme 3**. Synthesis of the $^{99m}$Tc-labeled complexes from the ferrocene precursors

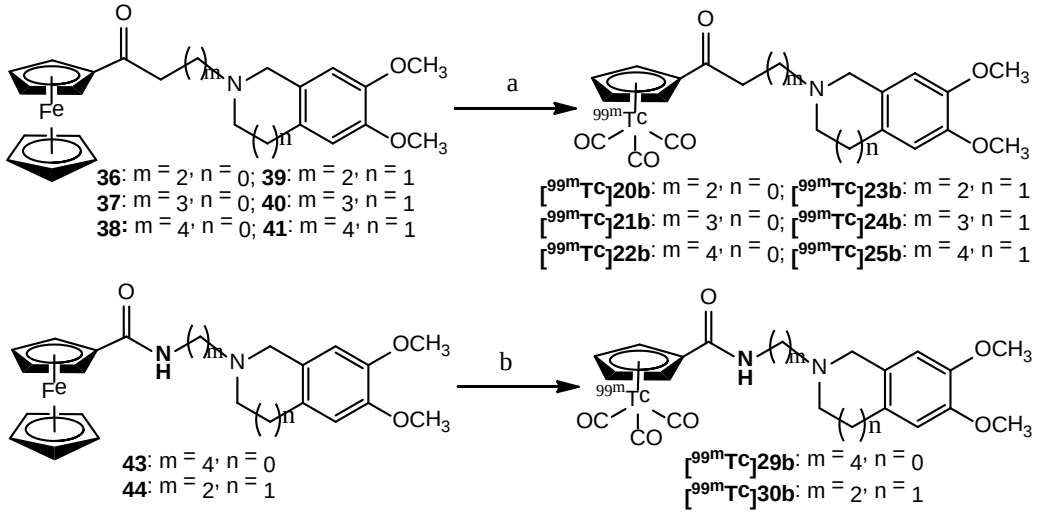


Reagents and conditions: (a) $^{99m}TcO_4^-$, $Mn(CO)_5$, DMF, 140 °C , 1 h, 13–32% for [$^{99m}$Tc]**20b**, 37–59% for [$^{99m}$Tc]**21b**, 25–33% for [$^{99m}$Tc]**22b**, 34–53% for [$^{99m}$Tc]**23b**, 44–62% for [$^{99m}$Tc]**24b**, 57–63% for [$^{99m}$Tc]**25b**; (b) $^{99m}TcO_4^-$, $Mn(CO)_5$, DMF, 150 °C, 1 h, 36–67% for [$^{99m}$Tc]**29b**, 48–60% for [$^{99m}$Tc]**30b**.

## *In vitro* evaluation of the $^{99m}$Tc-labeled complexes in DU145 prostate cells

It has been reported that DU145 prostate tumor cells exhibit high expression of both $\sigma_1$ and $\sigma_2$ receptors.[4] Considering the affinity and subtype selectivity for $\sigma_2$ receptors, uptake experiments with the radioligands [$^{99m}$Tc]**20b**, [$^{99m}$Tc]**23b,** [$^{99m}$Tc]**29b**–**30b** in DU145 prostate tumor cells were performed. The results are summarized in Figure 3.

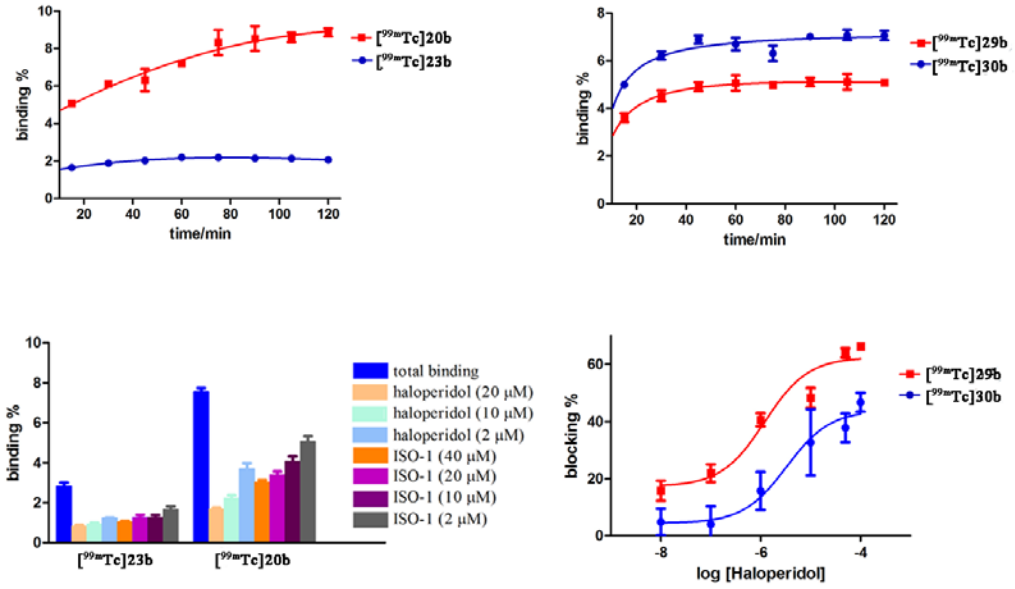


**Figure 3**. *In vitro* uptakes of [$^{99m}$Tc]**20b**, [$^{99m}$Tc]**23b**, [$^{99m}$Tc]**29b** and [$^{99m}$Tc]**30b** in DU145 prostate tumor cells.

After incubation for 120 min, the total uptake values of [$^{99m}$Tc]**20b** and [$^{99m}$Tc]**23b** were 8.86% and 2.06%, respectively. For the complexes with an amide group, the uptake values of [$^{99m}$Tc]**29b** and [$^{99m}$Tc]**30b** reached 4.91% and 6.89% at 45 min and increased slightly afterwards to 5.12% and 7.08% at 120 min, respectively. In blocking studies, treatment with haloperidol and ISO-1 significantly decreased the uptake values of [$^{99m}$Tc]**20b** and [$^{99m}$Tc]**23b** in a dose-dependent manner, indicating specific binding of [$^{99m}$Tc]**20b** and [$^{99m}$Tc]**23b** to $\sigma_2$ receptors in DU145 cells. Moreover, treatment with various concentrations of haloperidol led to decreased uptake of [$^{99m}$Tc]**29b** and [$^{99m}$Tc]**30b** in a dose-dependent manner. However, [$^{99m}$Tc]**29b** showed a higher blocking percentage than [$^{99m}$Tc]**30b** (66% *vs.* 47%) at the same concentration of haloperidol ($10^{-4}$ M), suggesting a higher specific binding of [$^{99m}$Tc]**29b** to σ receptors in DU145 cells.

### *In vitro* evaluation of the $^{99m}$Tc-labeled complexes in C6 glioma cells

C6 glioma tumor cells, with high expression of $\sigma_2$ receptors and low expression of $\sigma_1$ receptors,[3] were selected for further evaluation of [$^{99m}$Tc]**20b** and [$^{99m}$Tc]**29b**. The results are shown in Figure 4.

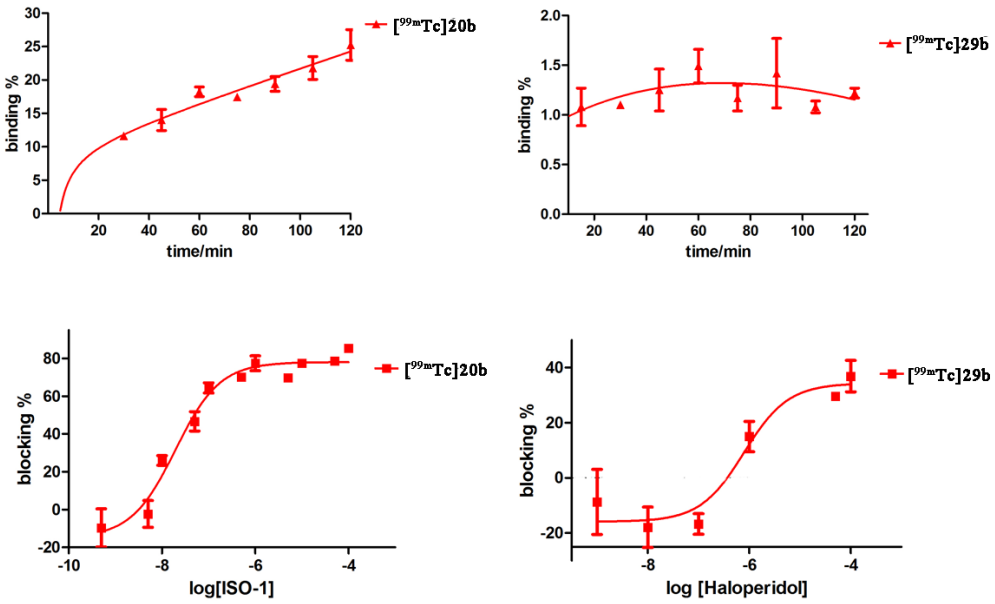


**Figure 4**. *In vitro* uptakes of [$^{99m}$Tc]**20b** and [$^{99m}$Tc]**29b** in C6 glioma cells.

High uptake of [$^{99m}$Tc]**20b** was observed in a time-dependent manner. The percentage of its uptake reached 25% after incubation for 120 min. Furthermore, coincubation with different concentrations of ISO-1 led to remarkably decreased uptake in a dose-dependent manner. The uptake was significantly reduced by about 80% with $10^{-6}$ M of ISO-1, suggesting high specific binding of [$^{99m}$Tc]**20b** to $\sigma_2$ receptors in C6 glioma cells. On the other hand, much lower uptake of [$^{99m}$Tc]**29b** (<1.49%) was observed. Treatment with different concentrations of haloperidol also led to reduction of [$^{99m}$Tc]**29b**. But the blocking percentage was low (37% with $10^{-4}$ M of haloperidol). In a word, [$^{99m}$Tc]**20b** displayed higher uptake and higher specific binding to $\sigma_2$ receptors than [$^{99m}$Tc]**29b** in C6 glioma cells.

Since compounds **21a** and **24a** had moderate to high affinity for $\sigma_2$ receptors, the uptake experiments of the corresponding [$^{99m}$Tc]**21b** and [$^{99m}$Tc]**24b** were performed

in C6 glioma cells. The results are provided in the Supporting Information (Figure S3). The total uptake of [$^{99m}$Tc]**21b** and [$^{99m}$Tc]**24b** were 4.88% and 5.12%, respectively. But treatment with $10^{-6}$ M of haloperidol only led to minimal reduction of the uptake, suggesting high nonspecific binding of [$^{99m}$Tc]**21b** and [$^{99m}$Tc]**24b** in C6 glioma cells.

### *In vivo* evaluation of the $^{99m}$Tc-labeled complexes

### Biodistribution and blocking studies in male ICR mice

To investigate the kinetics of the radiotracers, we performed biodistribution and blocking studies of [$^{99m}$Tc]**20b**, [$^{99m}$Tc]**23b**, [$^{99m}$Tc]**25b** and [$^{99m}$Tc]**29b** in ICR mice. The results are summarized in Tables 2–4, Figure 5 as well as in the Supporting Information (Table S7 and Figure S4). Both [$^{99m}$Tc]**20b** and [$^{99m}$Tc]**23b** exhibited high initial brain uptake with 2.57 ± 0.31 %ID/g and 2.38 ± 0.31 %ID/g at 2 min, respectively, and fast washout with 0.17 ± 0.04 %ID/g and 0.09 ± 0.01 %ID/g, respectively, at 240 min. On the other hand, [$^{99m}$Tc]**25b** exhibited lower brain uptake (1.05 ± 0.06 %ID/g) and relatively slow washout with 0.32 ± 0.04 %ID/g at 240 min. [$^{99m}$Tc]**20b**, [$^{99m}$Tc]**23b**, [$^{99m}$Tc]**25b** exhibited fast clearance from the blood and the muscle. Low accumulation in the blood of the above radiotracers was observed with 0.31 ± 0.04 % ID/g, 0.44 ± 0.15 %ID/g, and 0.30 ± 0.05 %ID/g at 240 min, respectively. Low accumulation in the muscle was also observed with 0.24 ± 0.11 % ID/g, 0.21 ± 0.07 %ID/g, and 0.49 ± 0.05 %ID/g at 240 min, respectively. In biodistribution studies of [$^{99m}$Tc]**29b** (Table 4), much lower brain uptake was observed with 0.24 ± 0.06 %ID/g at 2 min, indicating that the amide group had negative effect on the potential of the radiotracer to cross the BBB. Low accumulation of this radiotracer in the blood and the muscle at 240 min was observed.

**Table 2**. Biodistribution of [$^{99m}$Tc]**20b** in male ICR mice [a]

| Organ | 2 min | 15 min | 30 min | 60 min | 120 min | 240 min |
|---|---|---|---|---|---|---|
| Blood | 1.82 ± 0.18 | 0.81 ± 0.07 | 0.71 ± 0.07 | 0.57 ± 0.11 | 0.43 ± 0.07 | 0.31 ± 0.04 |
| Brain | 2.57 ± 0.31 | 2.70 ± 0.18 | 2.08 ± 0.22 | 1.06 ± 0.17 | 0.47 ± 0.08 | 0.17 ± 0.04 |
| Heart | 11.81 ± 1.58 | 3.25 ± 0.22 | 2.07 ± 0.23 | 1.31 ± 0.21 | 0.83 ± 0.14 | 0.43 ± 0.07 |
| Liver | 4.76 ± 1.29 | 10.03 ± 0.61 | 12.51 ± 1.88 | 13.41 ± 0.71 | 16.14 ± 1.73 | 17.33 ± 3.11 |
| Spleen | 3.43 ± 0.89 | 7.46 ± 0.81 | 7.15 ± 1.44 | 4.67 ± 0.38 | 2.76 ± 0.58 | 1.24 ± 0.36 |
| Lung | 29.38 ± 4.97 | 9.61 ± 2.58 | 7.14 ± 2.44 | 3.77 ± 0.80 | 2.19 ± 0.69 | 1.47 ± 0.53 |
| Kidney | 14.46 ± 1.08 | 15.48 ± 1.92 | 11.78 ± 1.04 | 8.92 ± 1.17 | 6.62 ± 0.99 | 6.11 ± 1.21 |
| Small intestine[b] | 4.07 ± 0.70 | 11.05 ± 1.77 | 11.69 ± 3.19 | 14.01 ± 2.20 | 15.08 ± 1.87 | 12.94 ± 2.36 |
| Stomach[b] | 0.96 ± 0.09 | 2.42 ± 0.74 | 2.67 ± 0.74 | 1.46 ± 0.40 | 1.56 ± 0.77 | 1.23 ± 0.26 |
| Muscle | 2.42 ± 0.78 | 2.16 ± 0.22 | 1.74 ± 0.20 | 1.40 ± 0.18 | 0.78 ± 0.23 | 0.24 ± 0.11 |
| Thyroid[b] | 0.20 ± 0.03 | 0.17 ± 0.05 | 0.17 ± 0.03 | 0.09 ± 0.02 | 0.12 ± 0.01 | 0.08 ± 0.03 |

[a]Data are expressed as percentage of injected dose per gram, means ± SD, n = 5.
[b]Percentage of injected dose per organ.

**Table 3**. Biodistribution of [$^{99m}$Tc]**23b** in male ICR mice [a]

| Organ | 2 min | 15 min | 30 min | 60 min | 120 min | 240 min |
|---|---|---|---|---|---|---|
| Blood | 2.11 ± 0.15 | 1.06 ± 0.09 | 0.89 ± 0.07 | 0.74 ± 0.06 | 0.54 ± 0.11 | 0.44 ± 0.15 |
| Brain | 2.38 ± 0.31 | 1.79 ± 0.20 | 1.08 ± 0.13 | 0.52 ± 0.02 | 0.20 ± 0.02 | 0.09 ± 0.01 |
| Heart | 8.73 ± 0.81 | 1.93 ± 0.13 | 1.29 ± 0.09 | 0.79 ± 0.09 | 0.51 ± 0.02 | 0.34 ± 0.02 |
| Liver | 7.51 ± 1.11 | 13.91 ± 0.92 | 17.03 ± 1.13 | 20.36 ± 1.30 | 22.63 ± 1.38 | 22.82 ± 3.22 |
| Spleen | 4.39 ± 1.34 | 5.59 ± 0.51 | 4.08 ± 0.48 | 2.64 ± 0.13 | 1.20 ± 0.23 | 0.66 ± 0.22 |
| Lung | 27.20 ± 5.00 | 7.13 ± 1.54 | 4.10 ± 1.23 | 2.67 ± 0.80 | 1.76 ± 0.40 | 1.29 ± 0.23 |
| Kidney | 18.88 ± 1.30 | 12.45 ± 1.30 | 9.91 ± 0.94 | 10.32 ± 1.37 | 9.86 ± 1.09 | 9.22 ± 1.82 |
| Small intestine[b] | 6.13 ± 1.02 | 8.75 ± 2.27 | 11.22 ± 1.74 | 15.53 ± 2.24 | 19.15 ± 2.63 | 15.89 ± 1.14 |
| Stomach[b] | 1.32 ± 0.29 | 2.54 ± 0.44 | 2.74 ± 0.24 | 3.27 ± 0.13 | 2.77 ± 0.45 | 1.58 ± 0.57 |
| Muscle | 2.67 ± 0.35 | 1.66 ± 0.23 | 1.22 ± 0.15 | 0.75 ± 0.11 | 0.38 ± 0.06 | 0.21 ± 0.07 |
| Thyroid[b] | 0.11 ± 0.05 | 0.18 ± 0.05 | 0.08 ± 0.01 | 0.11 ± 0.01 | 0.09 ± 0.04 | 0.07 ± 0.02 |

[a]Data are expressed as percentage of injected dose per gram, means ± SD, n = 5.
[b]Percentage of injected dose per organ.

**Table 4**. Biodistribution of [$^{99m}$Tc]**29b** in male ICR mice [a]

| Organ | 2 min | 15 min | 30 min | 60 min | 120 min | 240 min |
|---|---|---|---|---|---|---|
| Blood | 2.04 ± 0.29 | 0.74 ± 0.06 | 0.53 ± 0.03 | 0.43 ± 0.05 | 0.41 ± 0.04 | 0.34 ± 0.03 |
| Brain | 0.24 ± 0.06 | 0.21 ± 0.02 | 0.16 ± 0.02 | 0.11 ± 0.02 | 0.11 ± 0.01 | 0.10 ± 0.01 |
| Heart | 11.22 ± 1.20 | 3.27 ± 0.20 | 2.27 ± 0.24 | 1.74 ± 0.13 | 1.45 ± 0.20 | 1.01 ± 0.16 |
| Liver | 9.27 ± 1.69 | 18.56 ± 2.62 | 24.43 ± 1.60 | 27.13 ± 2.13 | 27.98 ± 2.32 | 28.45 ± 3.32 |
| Spleen | 5.08 ± 1.42 | 7.32 ± 0.65 | 4.50 ± 0.64 | 1.91 ± 0.58 | 1.21 ± 0.18 | 0.78 ± 0.12 |
| Lung | 31.54 ± 3.28 | 12.11 ± 2.08 | 8.93 ± 1.88 | 7.63 ± 2.40 | 4.17 ± 0.42 | 4.03 ± 0.54 |
| Kidney | 27.45 ± 4.91 | 17.68 ± 3.19 | 14.62 ± 0.61 | 12.14 ± 1.81 | 10.21 ± 0.51 | 8.79 ± 1.04 |
| Small intestine[b] | 6.00 ± 1.31 | 13.15± 1.09 | 10.62 ± 2.49 | 11.92 ± 3.25 | 22.56 ± 3.75 | 17.64 ± 4.15 |

| | | | | | | |
|---|---|---|---|---|---|---|
| Stomach[b] | 1.27 ± 0.32 | 2.59 ± 0.47 | 2.58 ± 1.16 | 2.17 ± 0.79 | 2.32 ± 0.92 | 1.46 ± 0.41 |
| Muscle | 4.12 ± 0.61 | 2.02 ± 0.16 | 1.44 ± 0.21 | 0.98 ± 0.13 | 0.68 ± 0.10 | 0.41 ± 0.03 |
| Thyroid[b] | 0.11 ± 0.02 | 0.08 ± 0.02 | 0.14 ± 0.03 | 0.09 ± 0.01 | 0.06 ± 0.01 | 0.05 ± 0.03 |

[a]Data are expressed as percentage of injected dose per gram, means ± SD, n = 5.
[b]Percentage of injected dose per organ.

To examine the specific binding of the radiotracers to σ receptors *in vivo*, blocking studies were carried out by administration of haloperidol (1.0 mg/kg) 5 min prior to the radiotracer administration. Pretreatment with haloperidol significantly reduced the accumulation of [$^{99m}$Tc]**20b**, [$^{99m}$Tc]**23b** and [$^{99m}$Tc]**29b** in the brain by 43%, 45%, and 36%**,** respectively, at 120 min postinjection (Figure 5). Moreover, remarkable reduction of radiotracers in the organs known to express σ receptors was observed, indicating specific binding of [$^{99m}$Tc]**20b**, [$^{99m}$Tc]**23b** and [$^{99m}$Tc]**29b** to σ receptors *in vivo*. However, there is no significant reduction of radiotracer accumulation observed in the brain for [$^{99m}$Tc]**25b** (Figure S4, in the Supporting Information), suggesting high nonspecific binding of [$^{99m}$Tc]**25b** *in vivo*.

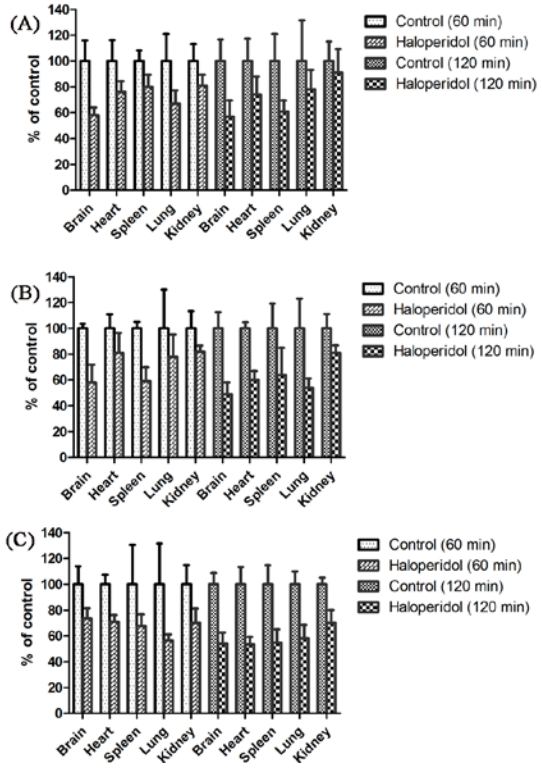


**Figure 5**. Effects of pretreatment with haloperidol (0.1 mL, 1.0 mg/kg) on organ biodistribution of [$^{99m}$Tc]**20b** (A), [$^{99m}$Tc]**23b** (B) or [$^{99m}$Tc]**29b** (C) in male ICR mice (n = 5). Student's *t* test (independent, two-tailed) was performed, and $p < 0.05$ (except for [$^{99m}$Tc]**20b** in the lungs and kidney 120 min after intravenous injection, [$^{99m}$Tc]**23b** in the heart and lungs 60 min after intravenous injection, and [$^{99m}$Tc]**29b** in the spleen 60 min after intravenous injection).

**Biodistribution and blocking studies of [$^{99m}$Tc]20b in Balb/c nude mice bearing C6 glioma xenografts**

Encouraged by the optimal properties of [$^{99m}$Tc]**20b** *in vitro* and *in vivo*, biodistribution and blocking studies of this radiotracer were performed in Balb/c mice bearing C6 glioma xenografts. The results are shown in Table 5 and Figure 6. High accumulation of radiotracer in the tumor was observed with 5.41 ± 0.91% ID/g at 120 min and 5.92 ± 1.30% ID/g at 240 min. At the same time, low accumulation of radiotracer in blood and muscle were observed as well. Therefore, high tumor/blood ratios and tumor/muscle ratios were obtained with 20.6 and 16.1 at 240 min, respectively. To further examine the specific binding to σ receptors in the tumor, blocking studies with haloperidol, ferrocene precursor **36** and siramesine as blocking agents were performed. Pretreatment of haloperidol, **36** and siramesine led to significant reduction of tumor accumulation by 33%, 62% and 44% at 240 min, respectively, indicating the specific binding of [$^{99m}$Tc]**20b** to σ receptors in the tumor. In addition, a reduction of radiotracer in the organs known to contain σ receptors such as brain, heart, and lung were observed, which is consistent with the biodistribution results in normal mice.

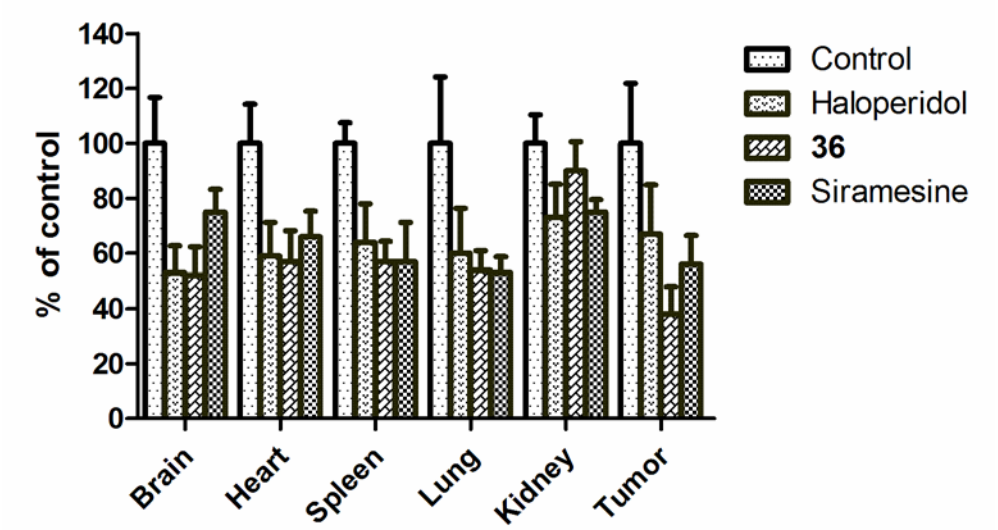


**Figure 6**. Effects of pretreatment with haloperidol, **36** and siramesine (0.1 mL, 1.0 mg/kg) on organ biodistribution of [$^{99m}$Tc]**20b** in Balb/c nude mice bearing C6 glioma xenografts. Student's *t* test (independent, two-tailed) was performed, and $p < 0.05$ (except in the kidney with **36** and in the tumor with haloperidol 240 min after intravenous injection).

**Table 5**. Biodistribution of [$^{99m}$Tc]**20b** in Balb/c nude mice bearing C6 glioma xenografts[a]

| Organ | 120 min | 240 min |
|---|---|---|
| Blood | 0.32 ± 0.05 | 0.28 ± 0.03 |
| Brain | 0.68 ± 0.21 | 0.30 ± 0.05 |
| Heart | 0.80 ± 0.09 | 0.55 ± 0.08 |
| Liver | 18.44 ± 3.58 | 22.47 ± 2.37 |
| Spleen | 5.48 ± 0.58 | 2.69 ± 0.20 |
| Lung | 2.92 ± 0.74 | 2.04 ± 0.49 |
| Kidney | 6.86 ± 1.16 | 5.93 ± 0.62 |
| Small intestine[b] | 15.26 ± 1.06 | 16.33 ± 3.12 |
| Stomach[b] | 0.82 ± 0.19 | 0.83 ± 0.34 |
| Muscle | 0.65 ± 0.11 | 0.37 ± 0.06 |
| Thyroid[b] | 0.08 ± 0.01 | 0.08 ± 0.01 |
| Tumor | 5.41 ± 0.91 | 5.92 ± 1.30 |
| Tumor/blood | 17.5 ± 4.0 | 20.6 ± 4.1 |
| Tumor/muscle | 8.5 ± 1.6 | 16.1 ± 5.3 |

[a]Data are expressed as percentage of injected dose per gram, means ± SD, n = 5.
[b]Percentage of injected dose per organ.

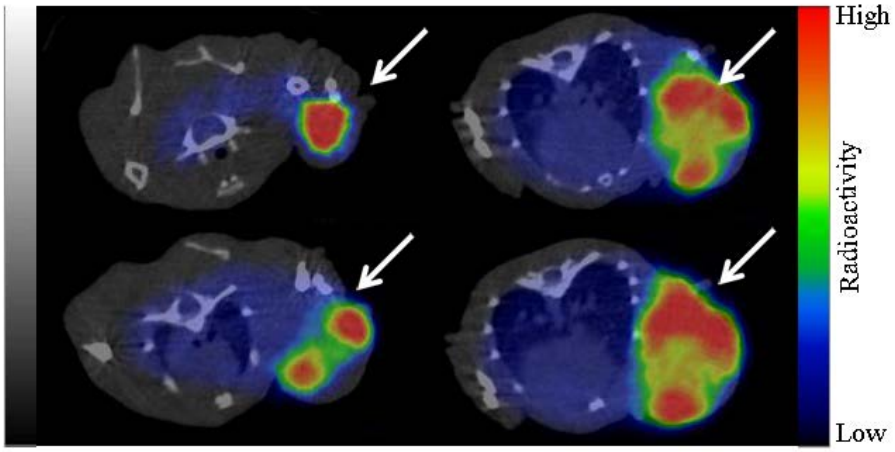


**Figure 7**. Representative transverse plane slices of NanoScan SPECT/CT fusion images of [$^{99m}$Tc]**20b** (22.2 MBq, 0.15 mL) in male Balb/c nude mouse bearing C6 glioma xenografts after 180 min postinjection. Isoflurane was used for anesthesia.

**Small animal SPECT/CT imaging of [$^{99m}$Tc]20b**

To further confirm the potential applications of [$^{99m}$Tc]**20b** in tumor imaging, small animal SPECT/CT scans of C6 glioma xenograft mouse model were performed using NanoScan□SPECT/CT. Representative transverse plane SPECT/CT images at 180 min postinjection of [$^{99m}$Tc]**20b** (22.2 MBq, 0.15 mL) are shown in Figure 7 and the coronal and sagittal plane images are shown in the Supporting Information (Figure S5). The solid tumor was clearly visualized with high tumor-to-background contrast, indicating that [$^{99m}$Tc]**20b** could determine the level of $\sigma_2$ receptors in solid tumors *in vivo*.

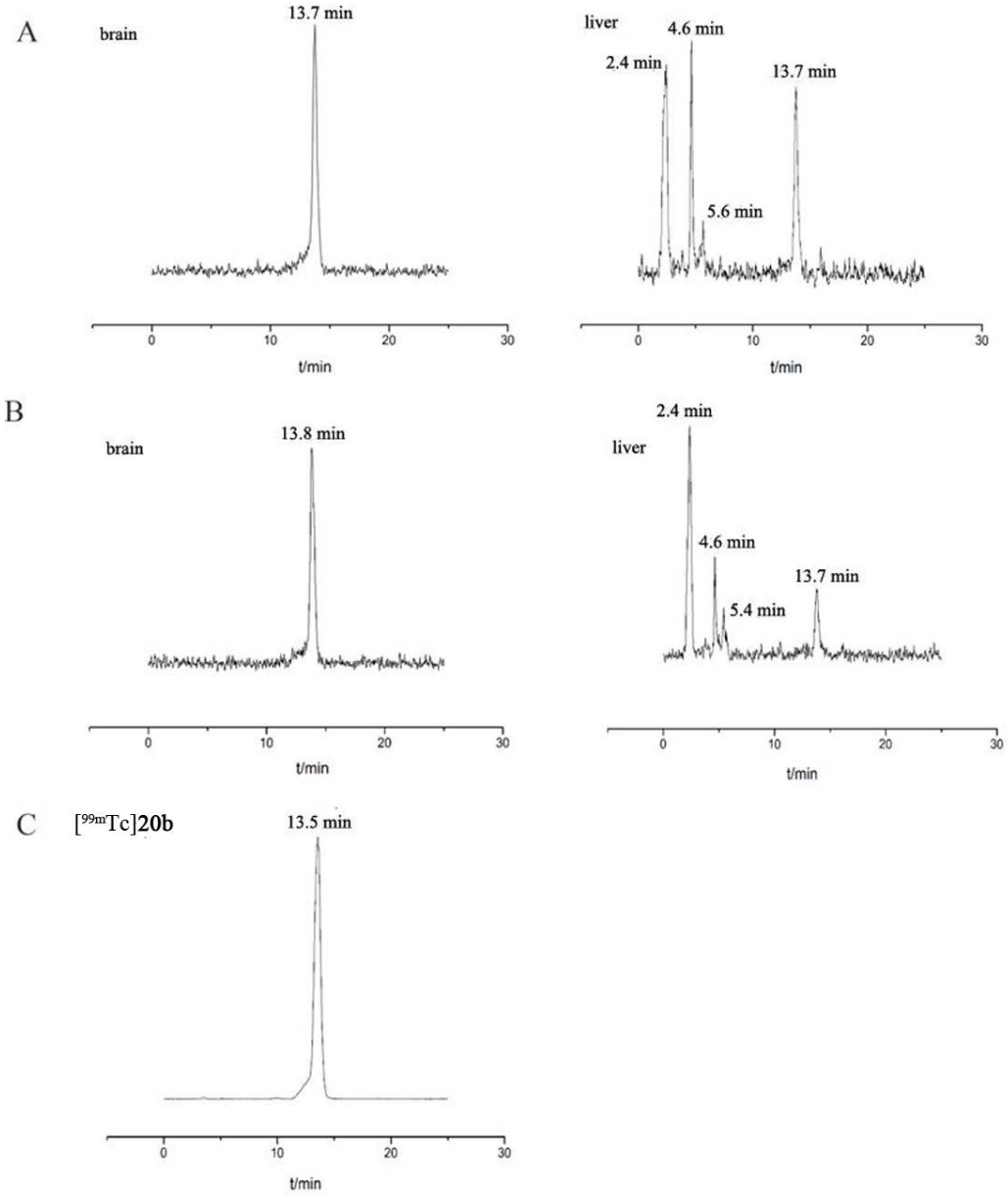


**Figure 8**. Analytical HPLC chromatograms of radioactive compounds in mouse brain and liver samples after intravenous injection of [$^{99m}$Tc]**20b** (18.5 MBq, 0.15 mL). (A) Brain and liver samples at 15 min. (B) Brain and liver samples at 30 min. (C) [$^{99m}$Tc]**20b.**

***In vivo* radiometabolic stability of [$^{99m}$Tc]20b**

The metabolic stability of [$^{99m}$Tc]**20b** was investigated in brain and liver samples of ICR mice 15 and 30 min after injection of the radiotracer. The HPLC chromatograms are shown in Figure 8. The parent radiotracer [$^{99m}$Tc]**20b** was the main radioactive compound presented in the brain at both 15 min and 30 min, indicating that [$^{99m}$Tc]**20b** was very stable in the brain and no entry of radioactive metabolites into the brain. In the liver samples, three main metabolites with retention times of 2.4 min (M1), 4.6 min (M2) and 5.4 min (M3), respectively, were observed. Furthermore, the percentage of the parent compound [$^{99m}$Tc]**20b** was decreased with the time (31.8% and 16.1% at 15 and 30 min, respectively). The percentage of M1 was significantly increased with 45.8% and 65.6% at 15 and 30 min, respectively.

## DISSCUSSION

A number of studies have demonstrated high expression of $\sigma_2$ receptors in many human tumors.[2-4] The $\sigma_2$ receptor has proved to be a unique biomarker of proliferative status in solid tumors.[7-9] Therefore, the development of molecular probes for imaging $\sigma_2$ receptors will provide useful information on the proliferative status of tumors in patients. Recently, [$^{18}$F]ISO-1 was developed as a potential $\sigma_2$ receptor PET radiotracer for imaging the proliferative status of tumors.[10-12] However, there is still a need for a $\sigma_2$ receptor SPECT imaging radioligands in clinical trials. $^{99m}$Tc is the most common and convenient nuclide for SPECT imaging in clinical use. Furthermore, $^{99m}$Tc/$^{188}$Re is considered as the ideal 'matched pair' of theragnostic radionuclides. Development of $^{99m}$Tc-labeled radiotracer will provide useful information of synthesis and therapeutic doses of the corresponding $^{188}$Re-labeled radiopharmaceuticals. Therefore, $^{99m}$Tc-labeled radiotracers for $\sigma_2$ receptors imaging could not only be used in the early diagnosis of cancer, but also could provide useful information for the therapeutic tumor medicine of $^{188}$Re-labeled radiopharmaceuticals. [$^{99m}$Tc][N-[2-((3′-N′-propyl-[3,3,1]aza-bicyclononan-3α-yl)(2″-methoxy-5-methyl-phenylcarbamate)(2-mercapttoethyl)amino)acetyl]-2-amino-ethanethiolato]technetium(V) oxide ([$^{99m}$Tc]**47)** was the most potential $\sigma_2$ receptor radiotracer ever reported with moderate affinity for $\sigma_2$ receptors ($K_i$ = 22 nM) and high subtype selectivity as well as visualization of tumor shape in planar gamma imaging.[18] But no further evaluation, such as SPECT/CT imaging, was reported since 2001. To the best of our knowledge, only the radiotracers with high tumor uptakes and high tumor-to-muscle ratios could have potential applications in the early diagnosis of tumor. Due to much higher expression of the $\sigma_2$ receptors in tumors and moderate to high expression of the $\sigma_1$ receptors in the normal organs, development of highly subtype selective $^{99m}$Tc-labeled $\sigma_2$ receptor radioligands with high tumor uptake and high tumor/background ratios will have wide applications in imaging proliferative status in solid tumors. Our aim in this paper is to develop novel $^{99m}$Tc-labeled radiotracers with high affinity for $\sigma_2$ receptors and high selectivity as well as clear visualization of solid tumor.

Enlightened by our previous results of $^{99m}$Tc-labeled radiotracers with the [(Cp-R)Tc(CO)$_3$] unit,[22,25] we replaced the aromatic ring of ISO-1 with [(Cp-R)M(CO)$_3$] unit with an electron-withdrawing group and connected it to 5,6-dimethoxyisoindoline or 6,7-dimethoxy-1,2,3,4-tetrahydroisoquinoline scaffold via different carbon length linkers. The designed complexes were in accordance with the $\sigma_2$ receptor ligand pharmacophore model proposed by Glennon with an amine binding site flanked by two hydrophobic regions.[37] It is encouraging that complexes

**20a**, **23a**, **29a**, and **30a** have high affinity and subtype selectivity for $\sigma_2$ receptors. Among these ligands, compound **20a** had low nanomolar affinity and higher subtype selectivity than ISO-1. Moreover, it showed high selectivity towards VAChT (2374-fold), dopamine $D_{2L}$ receptors, NMDA receptors, opiate receptors, DAT, NET, and SERT.

To detect the specific binding of the radiotracers to $\sigma_2$ receptors, we selected DU145 human prostate tumor cells ($B_{max}$ values of $\sigma_1$ and $\sigma_2$ receptors were 1800 and 1930 fmol/mg protein, respectively),[4] and C6 rat glioma cells ($B_{max}$ values of $\sigma_1$ and $\sigma_2$ receptors were 42 and 5507 fmol/mg protein, respectively).[3] In the *in vitro* uptake experiments in tumor cells, [$^{99m}$Tc]**20b** exhibited much higher uptake values and comparable specific binding to $\sigma_2$ receptors in DU145 cells than [$^{99m}$Tc]**23b**, which is in good agreement with the higher affinity of the former compound. Coincubation with ISO-1 led to significant reduction of uptake in a dose-dependent manner, indicating the specific binding of [$^{99m}$Tc]**20b** to $\sigma_2$ receptors. [$^{99m}$Tc]**29b** exhibited comparable uptake and higher specific binding to σ receptors in DU145 cells than [$^{99m}$Tc]**30b**. Thus, it seemed that the 5,6-dimethoxyisoindoline moiety is a better $\sigma_2$ preferring group than the 6,7-dimethoxy-1,2,3,4-tetrahydroisoquinoline moiety. In C6 glioma cells, [$^{99m}$Tc]**20b** displayed much higher uptake and higher specific binding to σ receptors than [$^{99m}$Tc]**29b**, indicating [$^{99m}$Tc]**20b** is the most potent radioligand in this series and warrants further evaluation.

To investigate the kinetics and examine the specific binding of the radiotracers *in vivo*, biodistribution studies of [$^{99m}$Tc]**20b**, [$^{99m}$Tc]**23b** and [$^{99m}$Tc]**29b** were performed in male ICR mice. [$^{99m}$Tc]**20b** and [$^{99m}$Tc]**23b** displayed high initial brain uptake with 2.57 and 2.38 %ID/g at 2 min postinjection, respectively. [$^{99m}$Tc]**29b** exhibited low brain uptake with 0.24 %ID/g at 2 min postinjection, indicating that the amide and carbonyl group showed different influence on the potential of the radiotracer to cross the BBB. Interestingly, all the radiotracers mentioned above exhibited fast clearance from the muscle and blood, which is very important for tumor imaging agents. Pretreatment with haloperidol significantly reduced the accumulation in the brain, indicating the specific binding of [$^{99m}$Tc]**20b**, [$^{99m}$Tc]**23b** and [$^{99m}$Tc]**29b** to σ receptors *in vivo*.

Finally, we selected the most potent radioligand [$^{99m}$Tc]**20b** and evaluated its potential applications in tumor imaging. In biodistribution studies in Balb/c nude mice bearing C6 glioma xenografts, [$^{99m}$Tc]**20b** showed much higher tumor uptake (5.41–5.92 % ID/g) than [$^{99m}$Tc]**47** (1.11–2.11% ID/g, 66 murine breast tumor)[18] and [$^{18}$F]ISO-1 (0.64–3.67% ID/g, EMT-6 mouse mammary tumor).[10] [$^{99m}$Tc]**20b** also exhibited fast clearance from the surrounding tissues. Thus, the tumor-to-muscle ratios (8.5–16.1) are higher than those of [$^{99m}$Tc]**47** (0.57–4.95) (16 *vs* 4.95 at 4 h).[18] Moreover, the tumor-to-blood ratios (17.5–20.6) are significantly higher than those of [$^{99m}$Tc]**47** (0.56–2.21)[18] and [$^{18}$F]ISO-1 (1.47–2.19).[10] Pretreatment with haloperidol, **36** and siramesine resulted in a remarkable reduction of radiotracer accumulation in the tumors, indicating specific binding of [$^{99m}$Tc]**20b** to σ receptors in C6 glioma tumors *in vivo*. Consistent with the high tumor uptakes and high tumor-to-muscle ratios in biodistribution studies, the animal SPECT/CT imaging of [$^{99m}$Tc]**20b** demonstrated a high uptake and clear visualization of C6 glioma xenografts in nude mice at 180 min. These data suggest the potential use of [$^{99m}$Tc]**20b** for SPECT imaging studies of brain tumors in patients.

## CONCLUSION

By applying an integrated strategy, we have designed, prepared and evaluated a series of cyclopentadienyl tricarbonyl $^{99m}$Tc/Re complexes containing 5,6-dimethoxyisoindoline or 6,7-dimethoxy-1,2,3,4-tetrahydroisoquinoline moiety. Compared with ISO-1, the rhenium complex of the corresponding radiotracer **20a** possessed higher affinity and subtype selectivity for $\sigma_2$ receptors. The corresponding radiotracer [$^{99m}$Tc]**20b** showed high uptakes and specific binding to σ receptors in DU145 prostate cells and C6 glioma cells. Moreover, [$^{99m}$Tc]**20b** exhibited high tumor uptake and high tumor/blood and tumor/muscle ratios in nude mice bearing C6 glioma xenografts. Furthermore, this radiotracer demonstrated specific binding to σ receptors in the tumor. In particular, animal SPECT/CT imaging studies with [$^{99m}$Tc]**20b** demonstrated a high uptake and clear visualization of C6 glioma xenografts in nude mice. These findings demonstrated the further evaluation of [$^{99m}$Tc]**20b** as a potential $\sigma_2$ receptor probe for imaging the proliferative status in brain tumors are worth doing.

## EXPERIMENTAL SECTION

All reagents used in the synthesis were commercial products and were used without further purification unless otherwise indicated. $^{99m}$Tc-pertechnetate was eluted from a commercial $^{99}$Mo–$^{99m}$Tc generator obtained from Beijing Atomic High-tech Co. The $^{1}$H NMR spectra were recorded on a Bruker Avance III NMR (400 MHz) spectrometers in $CDCl_3$ solutions at room temperature with TMS as an internal standard. Chemical shifts ($\delta$) were reported in ppm values relative to the internal TMS. Coupling constants ($J$) were reported in Hertz (Hz). Multiplicity is defined by s (singlet), d (doublet), t (triplet), and m (multiplet). The $^{13}$C NMR spectra were recorded on a Bruker Avance III NMR (100 MHz) spectrometers. Mass spectra were acquired by Quattro micro API ESI/MS (Waters, USA). High-resolution mass spectrometry (HRMS) was performed on a LCT Premier XE ESI-TOF mass spectrometry instrument (Waters, USA). X-ray crystallography data were collected on a Bruker Smart APEX II diffractometer (Bruker Co., Germany). Melting point (Mp) of solid compounds was tested on a WRX-4 micro melting point apparatus (Shanghai yice instrument Co., LTD, China) and was uncorrected. Reactions were monitored by TLC (TLC Silica gel 60 F254, Merck). Flash column chromatography was conducted using silica gel (45–75 μm) from Qingdao Haiyang Chemical Co., Ltd. The compounds were visualized by illumination with a short wavelength UV lamp (λ = 254 nm). High performance liquid chromatography (HPLC) separations and analyses were performed on a Waters 600 system (Waters, corporation, USA) equipped with a Waters 2489 UV–VIS detector and a Raytest Gabi NaI (Tl) scintillation detector (Raytest, Germany) and on a Shimadzu SCL-20AVP system (Shimadzu Corporation, Japan) equipped with a Bioscan Flow Count 3200 NaI/PMT γ-radiation scintillation detector. Samples were analyzed and separated on an Agela Venusil MP C18 column (250 mm × 4.6 mm, 5 μm) using acetonitrile with 0.1% trifluoroacetic acid (TFA) and water with 0.1% TFA as the mobile phase at a flow rate of 1 mL/min. All the final compounds were analyzed by HPLC with a purity of more than 95% (HPLC profiles are shown in the Supporting Information).

Male ICR mice (4–5 weeks, 22–25 g) were purchased from Vital River Laboratory Animal Technology Co. Ltd. All procedures related to animal experiments were performed in compliance with relevant laws and institutional guidelines. All protocols

requiring the use of mice were approved by the animal care committee of Beijing Normal University.

**Chemistry**

**2-(5,6-Dimethoxyisoindolin-2-yl)acetonitrile (5)**

Compound **3** (254.0 mg, 1.42 mmol) and 5 mL triethylamine was dissolved in 10 mL $CH_2Cl_2$, followed by addition of 2-bromoacetonitrile (200.0 mg, 1.67 mmol). The reaction mixture was stirred at room temperature for 24 h. The mixture was then washed with $H_2O$, and extracted with $CH_2Cl_2$. The organic layer was dried over $MgSO_4$, filtered, and concentrated under vacuum. The residue was purified by silica gel chromatography (dichloromethane: methanol = 100:1) to afford **5** (219.4 mg, 72%) as a white solid. Mp: 125.5–125.9 °C. $^1$H NMR (400 MHz, $CDCl_3$) $\delta$ 6.76 (s, 2H), 4.07 (s, 4H), 3.87 (s, 6H), 3.81 (s, 2H). ESI-MS: $[M + H]^+$ (m/z = 219.2).

**3-(5,6-Dimethoxyisoindolin-2-yl)propanenitrile** (**6**)

The procedure described for the synthesis of **5** was applied to compound **3** (251.2 mg, 1.40 mmol) and 3-bromopropanenitrile (223.7 mg, 1.67 mmol) to afford **6** (215.5 mg, 67%) as a light brown solid. Mp: 137.1–137.5 °C. $^1$H NMR (400 MHz, $CDCl_3$) $\delta$ 6.75 (s, 2H), 4.03 (s, 4H), 3.86 (s, 6H), 3.12 (t, $J$ = 7.0 Hz, 2H), 2.65 (t, $J$ = 6.4 Hz, 2H). ESI-MS: $[M + H]^+$ (m/z = 233.2).

**4-(5,6-Dimethoxyisoindolin-2-yl)butanenitrile** (**7**)

The procedure described for the synthesis of **5** was applied to **3** (254.5 mg, 1.42 mmol) and 4-bromobutanenitrile (247.2 mg, 1.67 mmol) to afford **7** (254.9 mg, 73%) as a light brown solid. $^1$H NMR (400 MHz, $CDCl_3$) $\delta$ 6.75 (s, 2H), 4.04 (s, 4H), 3.87 (s, 6H), 2.97 (t, $J$ = 6.7 Hz, 2H), 2.55 (t, $J$ = 7.1 Hz, 2H), 2.02 (t, $J$ = 6.7 Hz, 2H). ESI-MS: $[M + H]^+$ (m/z = 247.2).

**2-(5,6-Dimethoxyisoindolin-2-yl)ethanamine** (**11**)

A solution of $LiAlH_4$ (145.7 mg, 3.83 mmol) in 10 mL anhydrous diethyl ether was cooled at 0 °C (ice bath), followed by addition of a solution of **5** (210.0 mg, 0.96 mmol) in 5 mL of anhydrous THF. Then the reaction mixture was stirred at room temperature overnight. The reaction mixture was quenched with ice-$H_2O$ and extracted with ethyl acetate. The organic layer was dried over anhydrous $MgSO_4$, filtered, and concentrated under vacuum. The residue was purified by silica gel chromatography (dichloromethane: methanol: triethylamine = 20: 1: 1) to give **11** (97.2 mg, 46%) as a light yellow oil. $^1$H NMR (400 MHz, $CDCl_3$) $\delta$ 6.75 (s, 2H), 3.91 (s, 4H), 3.86 (s, 6H), 2.90–2.87 (m, 2H), 2.84–2.81 (m, 2H), 2.04 (br s, 2H). ESI-MS: $[M + H]^+$ (m/z = 223.2).

**3-(5,6-Dimethoxyisoindolin-2-yl)propan-1-amine** (**12**)

The procedure described for the synthesis of **11** was applied to $LiAlH_4$ (130.5 mg, 3.44 mmol) and compound **6** (200.0 mg, 0.86 mmol) to afford **12** (73.0 mg, 36%) as a brown oil. $^1$H NMR (400 MHz, $CDCl_3$) $\delta$ 6.75 (s, 2H), 4.07 (s, 4H), 3.83 (s, 6H), 3.15 (q, 2H, $J$ = 7.3 Hz), 1.74–1.67 (m, 2H), 1.47–1.32 (m, 2H). ESI-MS: $[M + H]^+$ (m/z = 237.2).

**4-(5,6-Dimethoxyisoindolin-2-yl)butan-1-amine** (**13**)

The procedure described for the synthesis of **11** was applied to $LiAlH_4$ (129.0 mg, 3.40 mmol) and compound **7** (210.0 mg, 0.85 mmol) to afford **13** (92.4 mg, 50%) as a brown oil. $^1$H NMR (400 MHz, $CDCl_3$) $\delta$ 6.73 (s, 2H), 4.81 (br s, 2H), 3.93 (s, 4H), 3.85 (s, 6H), 2.84–2.81 (m, 2H), 2.76 (m, 2H), 1.76–1.66 (m, 4H). ESI-MS: $[M + H]^+$ (m/z = 251.2).

**3-(5.6-Dimethoxyisoindolin-2-yl)-propylcarbonylcyclopentadienylTricarbonyl**

**Rhenium (20a)**

Compound **3** (23.0 mg, 0.13 mmol) was added to a solution of **17** (57.7 mg, 0.12 mmol) and KI (20.0 mg, 0.12 mmol) in 5 mL of toluene and 3 mL of triethylamine. The mixture was refluxed at 115 °C for 5 h. After cooled to room temperature, the solvent was evaporated in vacuum. The residue was purified by silica gel chromatography (ethyl acetate: petroleum ether: triethylamine = 1 : 3 : 1) to afford **20a** (8.6 mg, 10%) as a dark oil. $^{1}$H NMR (400 MHz, $CDCl_3$) $\delta$ 6.74 (s, 2H), 5.98 (t, $J$ = 2.2 Hz, 2H), 5.37 (t, $J$ = 2.2 Hz, 2H), 3.88 (s, 4H), 3.85 (s, 6H), 2.78–2.71 (m, 4H), 2.00–1.93 (m, 2H). $^{13}$C NMR (100 MHz, $CDCl_3$) $\delta$ 194.85, 191.91, 148.53, 131.52, 105.99, 96.61, 87.69, 85.11, 59.04, 56.19, 54.98, 36.36, 23.51. TOF-ES$^+$-MS, [M + H]$^+$: m/z calcd for $C_{22}H_{22}NO_6{}^{185}Re$ 582.1055; found 582.1045.

**4-(5.6-Dimethoxyisoindolin-2-yl)-butylcarbonylcyclopentadienyl Tricarbonyl Rhenium (21a)**

The procedure described for the synthesis of **20a** was applied to **18** (70 mg, 0.14 mmol) and **3** (51.9 mg, 0.29 mmol) to afford **21a** as a dark oil (12.8 mg, 10%). $^{1}$H NMR (400 MHz, $CDCl_3$) $\delta$ 6.74 (s, 2H), 5.99 (t, $J$ = 2.3 Hz, 2H), 5.36 (t, $J$ = 2.3 Hz, 2H), 3.94 (s, 4H), 3.85 (s, 6H), 2.79 (t, $J$ = 7.2 Hz, 2H), 2.66 (t, $J$ = 7.0 Hz, 2H), 1.84–1.77 (m, 2H), 1.70–1.62 (m, 2H). $^{13}$C NMR (100 MHz, $CDCl_3$) $\delta$ 194.74, 191.90, 148.66, 130.90, 105.95, 96.24, 87.82, 85.13, 59.10, 56.19, 55.93, 38.41, 29.70, 27.69, 22.00. HRMS (TOF-ES$^+$-MS): m/z calcd. for $C_{22}H_{24}NO_6{}^{185}Re$ [M + H]$^+$ 596.1212; found 596.1219.

**5-(5.6-Dimethoxyisoindolin-2-yl)-pentylcarbonylcyclopentadienyl Tricarbonyl Rhenium (22a)**

Compound **3** (31.9 mg, 0.18 mmol) was added to a solution of **19** (60.0 mg, 0.12 mmol), KI (32.1 mg, 0.19 mmol) and $K_2CO_3$ (25.0 mg, 0.18 mmol) in 10 mL anhydrous acetonitrile. The mixture was stirred at 90 °C for 5 h. After cooled to room temperature, the mixture was poured with cold water and extracted with $CH_2Cl_2$. The organic layer was dried over anhydrous $MgSO_4$, filtered, and concentrated under vacuum. The residue was purified by silica gel chromatography (ethyl acetate: petroleum ether: triethylamine = 1: 3: 1) to afford **22a** ( 29.8 mg, 41%) as a dark oil. $^{1}$H NMR (400 MHz, $CDCl_3$) $\delta$ 6.74 (s, 2H), 5.99 (t, $J$ = 2.2 Hz, 2H), 5.39 (t, $J$ = 2.2 Hz, 2H), 3.89 (s, 4H), 3.86 (s, 6H), 2.72 (t, $J$ = 7.4 Hz, 2H), 2.62 (t, $J$ = 7.3 Hz, 2H), 1.78–1.71 (m, 2H), 1.66–1.58 (m, 2H), 1.48–1.42 (m, 2H). $^{13}$C NMR (125 MHz, $CDCl_3$) $\delta$ 195.20, 191.88, 148.35, 131.71, 105.88, 96.51, 87.90, 85.18, 59.26, 56.13, 55.93, 38.78, 28.72, 26.93, 24.31. HRMS (TOF-ES$^+$-MS): m/z calcd. for $C_{24}H_{26}NO_6{}^{185}Re$ [M + H]$^+$ 610.1368; found 610.1362.

**3-(6,7-Dimethoxy-3,4-dihydro-1*H*-isoquinolin-2-yl)-propylcarbonylcyclopentadienyl Tricarbonyl Rhenium (23a)**

The procedure described for the synthesis of **20a** was applied to **17** (53.5 mg, 0.11 mmol) and **4** (32.0 mg, 0.16 mmol) to afford **23a** as a yellow oil (19.7 mg, 30%). $^{1}$H NMR (400 MHz, $CDCl_3$) $\delta$ 6.58 (s, 1H), 6.51 (s, 1H), 5.96 (t, $J$ = 2.2 Hz, 2H), 5.34 (t, $J$ = 2.2 Hz, 2H), 3.84 (s, 3H), 3.83 (s, 3H), 3.56 (s, 2H), 2.81–2.78 (m, 2H), 2.74–2.67 (m, 4H), 2.57 (t, $J$ = 6.8 Hz, 2H), 2.03–1.96 (m, 2H). $^{13}$C NMR (125 MHz, $CDCl_3$) $\delta$ 194.65, 191.90, 147.99, 147.58, 125.04, 111.31, 109.40, 96.15, 87.84, 85.25, 55.97, 55.95, 54.70, 50.23, 36.29, 29.71, 20.97. HRMS (TOF-ES$^+$-MS): m/z calcd. for $C_{22}H_{24}NO_6{}^{185}Re$ [M + H]$^+$ 596.1212; found 596.1215.

**4-(6,7-Dimethoxy-3,4-dihydro-1*H*-isoquinolin-2-yl)-butylcarbonylcyclopentadienyl Tricarbonyl Rhenium (24a)**

The procedure described for the synthesis of **20a** was applied to **18** (60 mg, 0.12 mmol) and **4** (50.1 mg, 0.26 mmol) to afford **24a** as a yellow oil (22 mg, 36%). $^{1}$H

NMR (400 MHz, $CDCl_3$) $\delta$ 6.59 (s, 1H), 6.52 (s, 1H), 6.00 (t, $J$ = 2.3 Hz, 2H), 5.33 (t, $J$ = 2.3 Hz, 2H), 3.84 (s, 3H), 3.83 (s, 3H), 3.58 (s, 2H), 2.83 (t, $J$ = 5.2 Hz, 2H), 2.74 (t, $J$ = 5.4 Hz, 2H), 2.65 (t, $J$ = 7.0 Hz, 2H), 2.56 (t, $J$ = 7.0 Hz, 2H), 1.82–1.74 (m, 2H), 1.73–1.63 (m, 2H). $^{13}$C NMR (100 MHz, $CDCl_3$) $\delta$ 195.10, 191.91, 147.59, 147.28, 126.65, 126.21, 111.46, 109.62, 96.18, 87.94, 85.08, 57.48, 55.96, 55.75, 50.91, 38.58, 29.71, 28.64, 26.29, 22.44. HRMS (TOF-ES$^+$-MS): m/z calcd. for $C_{22}H_{26}NO_6{}^{185}Re$ $[M + H]^+$ 610.1368; found 610.1366.

**5-(6,7-Dimethoxy-3,4-dihydro-1*H*-isoquinolin-2-yl)-pentylcarbonylcyclopentadienyl Tricarbonyl Rhenium (25a)**

The procedure described for the synthesis of **22a** was applied to **19** (78.5 mg, 0.15 mmol) and **4** (45.2 mg, 0.23 mmol) to afford **25a** as a colorless oil (48.6 mg, 51%). $^1$H NMR (400 MHz, $CDCl_3$) $\delta$ 6.59 (s, 1H), 6.52 (s, 1H), 5.98 (t, $J$ = 2.2 Hz, 2H), 5.38 (t, $J$ = 2.2 Hz, 2H), 3.84 (s, 3H), 3.83 (s, 3H), 3.55 (s, 2H), 2.82 (t, $J$ = 5.7 Hz, 2H), 2.70 (t, $J$ = 5.8 Hz, 2H), 2.61 (t, $J$ = 7.3 Hz, 2H), 2.51 (t, $J$ = 7.5 Hz, 2H), 1.77–1.69 (m, 2H), 1.68–1.59 (m, 2H), 1.45–1.37 (m, 2H). $^{13}$C NMR (125 MHz, $CDCl_3$) $\delta$ 195.20, 191.88, 147.47, 147.17, 126.73, 126.25, 111.36, 109.50, 96.15, 87.89, 85.18, 58.14, 55.92, 55.91, 55.86, 51.10, 38.79, 28.72, 27.10, 27.04, 24.32. HRMS (TOF-ES$^+$-MS): m/z calcd. for $C_{25}H_{28}NO_6{}^{185}Re$ $[M + H]^+$ 624.1525; found 624.1519.

**2-(5,6-Dimethoxyisoindolin-2-yl)-ethylaminocarbonylcyclopentadienyl Tricarbonyl Rhenium (27a)**

Under $N_2$, the solution of compound **11** (60.0 mg, 0.27 mmol) in 1.5 mL of anhydrous DMF and 100 μL of triethylamine was added to the solution of compound **26** (98.2 mg, 0.18 mmol) in 1 mL anhydrous DMF dropwise. The reaction mixture was stirred at room temperature for 4 h. The solvent was removed, washed with saturated sodium chloride and extracted with ethyl acetate. The organic layer was dried over anhydrous $MgSO_4$, filtered, and concentrated under vacuum. The residue was purified by silica gel chromatography (ethyl ether: hexane: triethylamine = 10: 5: 1) to afford **27a** (49.9 mg, 48%) as a pale yellow solid. Mp: 165.1–167.1 °C. $^1$H NMR (400 MHz, $CDCl_3$) $\delta$ 7.16 (br s, 1H), 6.76 (s, 2H), 6.04 (s, 2H), 5.34 (t, $J$ = 2.2 Hz, 2H), 4.12 (s, 4H), 3.87 (s, 6H), 3.61 (q, $J$ = 5.4 Hz, 2H), 3.07 (t, $J$ = 5.3 Hz, 2H).$^{13}$C NMR (100 MHz, $CDCl_3$) $\delta$ 192.58, 162.28, 148.64, 131.10, 105.93, 95.13, 86.03, 84.66, 58.99, 56.15, 54.36, 38.12. HRMS (EI): m/z calcd for $C_{21}H_{21}N_2O_6{}^{185}Re$ $[M + H]^+$ 583.1008, found 583.0995.

**3-(5,6-Dimethoxyisoindolin-2-yl)-propylaminocarbonylcyclopentadienyl Tricarbonyl Rhenium (28a)**

The procedure described for the synthesis of **27a** was applied to the compound **12** (40.0 mg, 0.17 mmol) and compound **26** (60.0 mg, 0.11 mmol) to afford **28a** (26.1 mg, 40%) as a pale yellow oil. $^1$H NMR (400 MHz, $CDCl_3$) $\delta$ 9.05 (br s, 1H), 6.82 (s, 2H), 5.48 (t, $J$ = 2.2 Hz, 2H), 5.10 (t, $J$ = 2.2 Hz, 2H), 3.97 (s, 4H), 3.88 (s, 6H), 3.53 (q, $J$ = 5.4 Hz, 2H), 3.03 (t, $J$ = 5.4 Hz, 2H), 1.84–1.78 (m, 2H).HRMS (EI): m/z calcd for $C_{22}H_{23}N_2O_6{}^{185}Re$ $[M + H]^+$ 597.1164, found 597.1177.

**4-(5,6-Dimethoxyisoindolin-2-yl)-butylaminocarbonylcyclopentadienyl Tricarbonyl Rhenium (29a)**

The procedure described for the synthesis of **27a** was applied to compound **13** (40.0 mg, 0.17 mmol) and compound **26** (81.8 mg, 0.15 mmol) to afford **29a** (34.4 mg, 38%) as a pale yellow oil. $^1$H NMR (400 MHz, $CDCl_3$) $\delta$ 8.14 (br s, 1H), 6.78 (s, 2H), 5.57 (t, $J$ = 2.0 Hz, 2H), 5.11 (t, $J$ = 2.2 Hz, 2H), 3.98 (s, 4H), 3.87 (s, 6H), 3.41 (q, $J$ = 4.9 Hz, 2H), 2.85 (t, $J$ = 5.4 Hz, 2H), 1.76–1.75 (m, 4H). $^{13}$C NMR (100 MHz, $CDCl_3$) $\delta$ 192.95, 162.03, 148.79, 131.16, 106.02, 96.86, 84.99, 84.57, 59.19, 56.17, 55.96, 39.71, 27.71, 26.81. HRMS (EI): m/z calcd for $C_{23}H_{25}N_2O_6{}^{185}Re$ $[M + H]^+$ 611.1321,

found 611.1323.

**2-(6,7-Dimethoxy-3,4-dihydroisoquinolin-2(1*H*)-yl)-ethylaminocarbonylcyclopentadienyl Tricarbonyl Rhenium (30a)**

The procedure described for the synthesis of **27a** was applied to compound **14** (74.4 mg, 0.32 mmol) and compound **26** (85.0 mg, 0.16 mmol) to afford **30a** as a light yellow solid (70.4 mg, 74%). Mp: 133.6–134.9 °C. $^{1}$H NMR (400 MHz, $CDCl_3$) $\delta$ 6.62 (s, 1H), 6.53 (s, 1H), 5.96 (s, 2H), 5.33 (t, $J$ = 2.2 Hz, 2H), 3.85 (d, $J$ = 6.3 Hz, 6H), 3.66 (s, 2H), 3.58 (q, $J$ = 5.1 Hz, 2H), 2.90 (s, 4H), 2.81 (s, 2H).$^{13}$C NMR (100 MHz, $CDCl_3$) $\delta$ 192.57, 162.19, 147.76, 147.41, 125.89, 125.83, 111.46, 109.54, 95.17, 85.98, 84.66, 56.09, 55.95, 55.93, 55.26, 50.64, 36.32, 28.40, 26.89. HRMS (EI): m/z calcd for $C_{22}H_{23}N_2O_6{}^{185}Re$ $[M + H]^+$ 597.1164, found 597.1176.

**3-(6,7-Dimethoxy-3,4-dihydroisoquinolin-2(1*H*)-yl)-propylaminocarbonylcyclopentadienyl Tricarbonyl Rhenium** (**31a**)

The procedure described for the synthesis of **27a** was applied to compound **15** (70.2 mg, 0.28 mmol) and compound **26** (82.7 mg, 0.15 mmol) to afford **31a** as a light yellow solid (67.6 mg, 74%). Mp: 123.6–124.5 °C. $^{1}$H NMR (400 MHz, $CDCl_3$) $\delta$ 6.65 (s, 1H), 6.59 (s, 1H), 5.39 (s, 2H), 5.01 (t, $J$ = 2.0 Hz, 2H), 3.86 (d, $J$ = 8.0 Hz, 6H), 3.66 (s, 2H), 3.51 (q, $J$ = 5.2 Hz, 2H), 2.97 (t, $J$ = 5.8 Hz, 2H), 2.86 (t, $J$ = 5.5 Hz, 2H), 2.79 (t, $J$ = 5.2 Hz, 2H), 1.83 (t, $J$ =4.7 Hz, 2H).$^{13}$C NMR (100 MHz, $CDCl_3$) $\delta$ 192.94, 161.69, 148.20, 147.62, 126.10, 125.90, 111.44, 109.89, 96.33, 84.93, 84.52, 56.08, 55.96, 55.42, 51.78, 41.31, 28.89, 23.86. HRMS (EI): m/z calcd for $C_{23}H_{25}N_2O_6{}^{185}Re$ $[M + H]^+$ 611.1321, found 611.1323.

**4-(6,7-Dimethoxy-3,4-dihydroisoquinolin-2(1*H*)-yl)-butylaminocarbonylcyclopentadienyl Tricarbonyl Rhenium** (**32a**)

The procedure described for the synthesis of **27a** was applied to compound **16** (89.0 mg, 0.34 mmol) and compound **26** (85.9 mg, 0.16 mmol) to afford **32a** as a light yellow oil (67.6 mg, 83%). $^{1}$H NMR (400 MHz, $CDCl_3$) $\delta$ 7.55 (br s, 1H), 6.63 (s, 1H), 6.56 (s, 1H), 5.58 (s, 2H), 5.07 (t, $J$ = 2.2 Hz, 2H), 3.85 (d, $J$ = 2.4 Hz, 6H), 3.65 (s, 2H), 3.41 (q, $J$ = 5.6 Hz, 2H), 2.90 (t, $J$ = 5.8 Hz, 2H), 2.80 (t, $J$ = 5.6 Hz, 2H), 2.63 (t, $J$ = 6.0 Hz, 2H), 1.79–1.68 (m, 4H). $^{13}$C NMR (100 MHz, $CDCl_3$) $\delta$ 192.92, 161.83, 147.83, 147.40, 126.26, 126.15, 111.49, 109.50, 96.02, 85.46, 84.55, 57.11, 56.66, 55.92, 50.01, 39.22, 28.52, 27.37, 24.69. HRMS (EI): m/z calcd for $C_{24}H_{27}N_2O_6{}^{185}Re$ $[M + H]^+$ 625.1477, found 625.1483.

**3-(5,6-Dimethoxyisoindolin-2-yl)-propylcarbonylferrocene (36)**

The procedure described for the synthesis of **20a** was applied to **33** (97.5 mg, 0.29 mmol) and **3** (75.9 mg, 0.42 mmol) to afford **36** as an orange solid (20.5 mg, 16%). Mp: 116.5–119.4 °C. $^{1}$H NMR (400 MHz, $CDCl_3$) $\delta$ 6.75 (s, 2H), 4.81 (t, $J$ = 1.7 Hz, 2H), 4.49 (t, $J$ = 1.7 Hz, 2H), 4.20 (s, 5H), 3.94 (s, 4H), 3.86 (s, 6H), 2.88–2.80 (m, 4H), 2.04–1.98 (m, 2H). ESI-MS: $[M + H]^+$ (m/z = 434.6).

**4-(5,6-Dimethoxyisoindolin-2-yl)-butylcarbonylferrocene (37)**

The procedure described for the synthesis of **20a** was applied to **34** (91.3 mg, 0.26 mmol) and **3** (107.5 mg, 0.60 mmol) to afford **37** as an orange solid (25.8 mg, 19%). Mp: 105.6–107.4 °C. $^{1}$H NMR (400 MHz, $CDCl_3$) $\delta$ 6.74 (s, 2H), 4.81 (t, $J$ = 1.9 Hz, 2H), 4.49 (t, $J$ = 1.8 Hz, 2H), 4.20 (s, 5H), 3.91 (s, 4H), 3.86 (s, 6H), 2.79–2.75 (m, 4H), 1.85–1.78 (m, 2H), 1.71–1.63 (m, 2H). ESI-MS: $[M + H]^+$ (m/z = 447.9).

**5-(5,6-Dimethoxyisoindolin-2-yl)-pentylcarbonylferrocene (38)**

The procedure described for the synthesis of **22a** was applied to **35** (49.3 mg, 0.14 mmol) and **3** (25.1 mg, 0.14 mmol) to afford **38** as an orange solid (56.5 mg, 44%). Mp: 108.1–110.0 °C. $^{1}$H NMR (400 MHz, $CDCl_3$) $\delta$ 6.75 (s, 2H), 4.78 (t, $J$ = 1.9 Hz, 2H), 4.49 (t, $J$ = 1.9 Hz, 2H), 4.20 (s, 5H), 3.95 (s, 4H), 3.86 (s, 6H), 2.79 (s, 2H),

2.74 (t, *J* = 7.4 Hz, 2H), 1.81–1.73 (m, 2H), 1.69 (s, 2H), 1.53–1.45 (m, 2H). ESI-MS: $[M + H]^+$ (m/z = 462.18).

**3-(6,7-Dimethoxy-3,4-dihydro-1*H*-isoquinolin-2-yl)-propylcarbonylferrocene (39)**

The procedure described for the synthesis of **20a** was applied to **33** (85.8 mg, 0.26 mmol) and **4** (62.1 mg, 0.32 mmol) to afford **39** as an orange solid (34.3 mg, 33%). Mp: 114.1–116.1 °C. $^1$H NMR (400 MHz, $CDCl_3$) $\delta$ 6.60 (s, 1H), 6.53 (s, 1H), 4.79 (t, *J* = 1.9 Hz, 2H), 4.48 (t, *J* = 1.9 Hz, 2H), 4.19 (s, 5H), 3.84 (s, 3H), 3.83 (s, 3H), 3.61 (s, 2H), 2.83 (t, *J* = 7.1 Hz, 2H), 2.77 (s, 2H), 2.63 (s, 2H), 2.04–2.01 (m, 2H). ESI-MS: $[M + H]^+$ (m/z = 448.7).

**4-(6,7-Dimethoxy-3,4-dihydro-1*H*-isoquinolin-2-yl)-butylcarbonylferrocene (40)**

The procedure described for the synthesis of **20a** was applied to **34** (102.6 mg, 0.29 mmol) and **4** (116.0 mg, 0.60 mmol) to afford **40** as an orange oil (25.7 mg, 22%). $^1$H NMR (400 MHz, $CDCl_3$) δ 6.59 (s, 1H), 6.53 (s, 1H), 4.79 (t, *J* = 1.9 Hz, 2H), 4.49 (t, *J* = 1.9 Hz, 2H), 4.19 (s, 5H), 3.84 (s, 3H), 3.83 (s, 3H), 3.59 (s, 2H), 2.84 (t, *J* = 5.6 Hz, 2H), 2.78–2.73 (m, 4H), 2.57 (t, *J* = 7.4 Hz, 2H), 1.81–1.70 (m, 4H). ESI-MS: $[M + H]^+$ (m/z = 461.9).

**5-(6,7-Dimethoxy-3,4-dihydro-1*H*-isoquinolin-2-yl)-pentylcarbonylferrocene (41)**

The procedure described for the synthesis of **22a** was applied to **35** (50.3 mg, 0.14 mmol) and **4** (34.1 mg, 0.18 mmol) to afford **41** as an orange solid (152.8 mg, 78%). Mp:118.6–120.8 °C $^1$H NMR (400 MHz, $CDCl_3$) $\delta$ 6.59 (s, 1H), 6.53 (s, 1H), 4.78 (t, *J* = 1.9 Hz, 2H), 4.49 (t, *J* = 1.8 Hz, 2H), 4.20 (s, 5H), 3.84 (s, 3H), 3.83 (s, 3H), 2.84 (s, 2H), 2.73 (t, *J* = 7.4 Hz, 2H), 2.55 (s, 2H), 1.80–1.72 (m, 2H), 1.68 (s, 2H), 1.49–1.42 (m, 2H). ESI-MS: $[M + H]^+$ (m/z = 476.2).

**4-(5,6-Dimethoxyisoindolin-2-yl)-butylaminocarbonylferrocene (43)**

Under $N_2$, the solution of compound **13** (66.0 mg, 0.26 mmol) in 1.5 mL of anhydrous DMF and 100 μL of triethylamine was added to the solution of compound **42** (102.9 mg, 0.26 mmol) in 1 mL anhydrous DMF dropwise. The reaction mixture was stirred at room temperature for 4 h. The solvent was removed, then washed with saturated sodium chloride and extracted with ethyl acetate. The organic layer was dried over anhydrous $MgSO_4$, filtered, and concentrated under vacuum. The residue was purified by silica gel chromatography (ethyl ether: hexane: triethylamine = 10: 5: 1) to afford **43** (78.4 mg, 65%) as a yellow solid. Mp: 119.6–120.4 °C. $^1$H NMR (400 MHz, $CDCl_3$)$\delta$ 6.76 (s, 2H), 6.62 (br s, 1H), 4.61 (s, 2H), 4.25 (s, 2H), 4.16 (s, 5H), 4.00 (s, 4H), 3.87 (s, 6H), 3.44 (d, *J* = 5.4 Hz, 2H), 2.86 (s, 2H), 1.74–1.70 (m, 4H).$^{13}$C NMR (100 MHz, $CDCl_3$) $\delta$ 170.12, 148.68, 131.14, 130.90, 105.99, 70.13, 69.67, 68.07, 65.55, 59.20, 56.20, 55.62, 39.33, 27.72, 26.33. HRMS (EI): m/z calcd for $C_{25}H_{31}N_2O_3Fe$ $[M + H]^+$463.1684, found 463.1686.

**2-(6,7-Dimethoxy-3,4-dihydroisoquinolin-2(1*H*)-yl)-ethylaminocarbonylferrocene (44)**

The procedure described for the synthesis of **43** was applied to compound **14** (38.0 mg, 0.16 mmol) and compound **42** (53.8 mg, 0.14 mmol) to afford **44** (49.8 mg, 69%) as a light yellow solid. Mp: 193.9–195.1 °C. $^1$H NMR (400 MHz, $CDCl_3$) $\delta$ 6.62 (s, 1H), 6.55 (s, 1H), 6.48 (br s, 1H), 4.66 (s, 2H), 4.30 (t, *J* = 1.8 Hz, 2H), 4.15 (s, 5H), 3.84 (d, *J* = 9.8 Hz, 6H), 3.68 (s, 2H), 3.59 (q, *J* = 5.4 Hz, 2H), 2.89–2.84 (m, 4H), 2.78 (t, *J* = 5.6 Hz, 2H).$^{13}$C NMR (100 MHz, $CDCl_3$) $\delta$ 170.35, 147.68, 147.38, 126.12, 125.99, 111.43, 109.47, 70.24, 69.68, 68.18, 56.64, 55.96, 55.94, 55.36, 50.91, 36.19, 28.71. HRMS (EI): m/z calcd for $C_{24}H_{29}N_2O_3Fe$ $[M + H]^+$ 449.1528, found 449.1520.

**3-(6,7-Dimethoxy-3,4-dihydroisoquinolin-2(1*H*)-yl)-propylaminocarbonylferrocene (45)**

The procedure described for the synthesis of **43** was applied to compound **15** (100.0 mg, 0.40 mmol) and compound **42** (158.4 mg, 0.40 mmol) to afford **45** (116.6 mg, 63%) as an orange solid. Mp: 72.2–73.6 °C. $^1$H NMR (400 MHz, $CDCl_3$) $\delta$ 7.73 (br s, 1H), 6.66 (s, 1H), 6.57 (s, 1H), 4.40 (s, 2H), 4.10 (s, 2H), 4.09 (s, 5H), 3.89 (s, 3H), 3.84 (s, 3H), 3.68 (s, 2H), 3.53 (q, $J$ = 5.4 Hz, 2H), 2.94 (t, $J$ = 5.9 Hz, 2H), 2.86–2.84 (m, 2H), 2.77 (t, $J$ = 5.6 Hz, 2H), 1.89–1.84 (m, 2H).$^{13}$C NMR (100 MHz, $CDCl_3$) $\delta$ 170.02, 147.88, 147.42, 126.36, 126.04, 111.43, 109.62, 69.99, 69.54, 67.86, 58.13, 56.04, 55.94, 55.79, 51.54, 40.32, 28.83, 25.19. ESI-MS: $[M + H]^+$ (m/z = 462.8).

**4-(6,7-Dimethoxy-3,4-dihydroisoquinolin-2(1*H*)-yl)-butylaminocarbonylferrocene** (**46**)

The procedure described for the synthesis of **43** was applied to compound **16** (36.7 mg, 0.14 mmol) and compound **42** (63.0 mg, 0.16 mmol) to afford **46** (45.0 mg, 68%) as an orange solid. Mp: 86.3–87.8 °C. $^1$H NMR (400 MHz, $CDCl_3$) $\delta$ 6.61 (s, 1H), 6.52 (s, 1H), 4.59 (s, 2H), 4.25 (t, $J$ = 1.8 Hz, 2H), 4.17 (s, 5H), 3.84 (d, $J$ = 9.8 Hz, 6H), 3.62 (s, 2H), 3.43 (q, $J$ = 6.2 Hz, 2H), 2.87 (d, $J$ = 5.4 Hz, 2H), 2.79 (d, $J$ = 5.1 Hz, 2H), 2.61 (t, $J$ = 6.1 Hz, 2H), 1.76–1.68 (m, 4H). $^{13}$C NMR (100 MHz, $CDCl_3$) $\delta$ 170.04, 147.64, 147.29, 126.46, 126.17, 111.42, 109.56, 70.17, 69.66, 68.03, 57.52, 56.03, 55.94, 50.76, 39.31, 28.60, 27.79, 24.69. HRMS (EI): m/z calcd for $C_{26}H_{33}N_2O_3Fe$ $[M + H]^+$ 477.1841, found 477.1833.

**X-ray Crystallography**

All the procedures for the X-ray crystallography were previously described.[36] Detailed procedures are shown in the Supporting Information.

***In vitro* radioligand competition studies**

**σ Receptor Binding Assays.** All the procedures for the radioligand competition studies were previously described.[20] Detailed procedures are shown in the Supporting Information.

**VAChT Binding Assays**. The determination of the affinity for VAChT were conducted by the method in the literatures.[38] Detailed procedures are shown in the Supporting Information.

**Dopamine $D_{2L}$ receptors**, **NMDA receptors**, **Opiate receptors**, **DAT**, **NET and SERT binding assay.** The affinities of compound **20a** for the above receptors and transporters are presented in percentage of inhibition form. The detailed information is shown in the Supporting Information.

**Radiochemistry**

The $^{99m}$Tc-pertechnetate was eluted from a commercial $^{99}$Mo–$^{99m}$Tc generator obtained from Beijing Atomic High-tech Co. The reactions were performed according to the methods in the literature.[22,25,39] Detailed procedures are provided in the Supporting Information.

**Measurement of log *D* values**

The log *D* values of [$^{99m}$Tc]**20b−25b** and [$^{99m}$Tc]**29b−30b** were determined by measuring the distribution of the radiotracer between 1-octanol and 0.05 mol/L sodium phosphate buffer at pH 7.4 according to literature.[22,25,36] Detailed procedures are provided in the Supporting Information.

***In vitro* evaluation in DU145 prostate cells and C6 glioma cells**

The culture of cells and the *in vitro* cell uptake and blocking assays were

performed as previously reported.[22,25] Detailed procedures are shown in the Supporting Information.

**Biodistribution and blocking studies in mice**

All animal experiments in ICR mice (n = 5, 4–5 weeks, 22–25 g) were performed in compliance with the national laws related to the care and experiments on laboratory animals. Biodistribution studies and blocking studies of HPLC-purified [$^{99m}$Tc]**20b**, [$^{99m}$Tc]**23b**, [$^{99m}$Tc]**25b**, [$^{99m}$Tc]**29b** (370 kBq, 0.1 mL) were carried out based on the method reported previously.[22,25] Detailed procedures are shown in the Supporting Information.

**Biodistribution and blocking studies of [$^{99m}$Tc]20b in Balb/c nude mice bearing C6 glioma xenografts**

All animal experiments in Balb/c nude mice (n = 4) were performed in compliance with the national laws related to the care and experiments on laboratory animals. Biodistribution studies and blocking studies of [$^{99m}$Tc]**20b** (370 kBq, 0.1 mL) were carried out based on the method reported previously.[25] Detailed procedures are shown in the Supporting Information.

**Small animal NanoScan SPECT/CT imaging of [$^{99m}$Tc]20b**

The detailed procedures of small animal imaging studies of [$^{99m}$Tc]**20b** (22.2 MBq, 0.15 mL) in male Balb/c nude mouse bearing C6 glioma xenografts are shown in the Supporting Information.

***In Vivo* Radiometabolic Stability of [$^{99m}$Tc]20b**

The *in vivo* metabolism of [$^{99m}$Tc]**20b** (18.5 MBq, 0.15 mL) was studied in male ICR mice according to the previously reported method.[36] Detailed procedures are shown in the Supporting Information.

## ASSOCIATED CONTENT

### Supporting Information

The general information and some parts of evaluation of the radiotracers in experimental section, purity of key target compounds, the HPLC chromatograms of **20a**−**25a** and [$^{99m}$Tc]**20b**−**25b**, **29a**−**30a** and [$^{99m}$Tc]**29b**−**30b**, X-ray crystallographic data for compound **31a,** *in vitro* evaluation of [$^{99m}$Tc]**21b** and [$^{99m}$Tc]**24b** in C6 glioma tumor cell line, biodistribution and blocking studies of [$^{99m}$Tc]**25b** in male ICR mice, small animal NanoScan SPECT/CT imaging of [$^{99m}$Tc]**20b**. This material is available free of charge via the Internet at http://pubs.acs.org.

## AUTHOR INFORMATION

### Corresponding Author

*To whom correspondence should be addressed: Phone: +86-10-58808891, Fax: +86-10-58808891. E-mail: hmjia@bnu.edu.cn

## ACKNOWLEDGMENTS

We give special thanks to Prof. Robert H. Mach for his helpful suggestions and

valuable comments on this manuscript. We are grateful to Dr. Xuebing Deng (College of Chemistry, Beijing Normal University) for his assistance with the X-ray diffraction. This work was supported by the National Natural Science Foundation of China (No. 21471019).

## ABBREVIATIONS

CNS, central nervous system; CPM, counts per minute; DLT, double ligand transfer; DMF, dimethylformamide; DTG, 1,3-di-*o*-tolyl-guanidine; [$^{18}$F]ISO-1, *N*-(4-(6,7-dimethoxy-3,4-dihydroisoquinolin-2(1*H*)-yl)butyl)-2-(2-[$^{18}$F]fluoroethoxy)-5-methylbenzamide; FBS, fetal bovine serum; BBB, blood-brain barrier; HPLC, high performance liquid chromatography; ID, injected dose; PET, positron emission tomography; rt, room temperature; SD, standard deviation; SPECT, single photon emission computed tomography; TFA, trifluoroacetic acid; THF, tetrahydrofuran; TLC, thin layer chromatography; VAChT, vesicular acetylcholine transporter.

## REFERENCES

1. Bading, J. R.; Shields, A. F. Imaging of cell proliferation: status and prospects. *J. Nucl. Med.* **2008**, 49, 64S-80S.
2. Bem, W. T.; Thomas, G. E.; Mamone, J. Y.; Homan, S. M.; Levy, B. K.; Johnson, F. E.; Coscia, C. J. Overexpression of σ receptors in nonneural human tumors. *Cancer Res.* **1991,** 51, 6558-6562.
3. Vilner, B. J.; John, C. S.; Bowen, W. D. Sigma-1 and sigma-2 receptors are expressed in a wide variety of human and rodent tumor cell lines. *Cancer Res.* **1995,** 55, 408-413.
4. John, C. S.; Vilner, B. J.; Geyer, B. C.; Moody, T.; Bowen, W. D. Targeting sigma receptor-binding benzamides as *in vivo* diagnostic and therapeutic agents for human prostate tumors. *Cancer Res.* **1999,** 59, 4578-4583.
5. van Waarde, A.; Rybczynska, A. A.; Ramakrishnan, N. K.; Ishiwata, K.; Elsinga, P. H.; Dierckx, R. A. J. O. Sigma receptors in oncology: therapeutic and diagnostic applications of sigma ligands. *Curr. Pharm. Des.* **2010,** 16, 3519-3537.
6. Megalizzi, V.; Le Mercier, M.; Decaestecker, C. Sigma receptors and their ligands in cancer biology: overview and new perspectives for cancer therapy. *Med. Res. Rev.* **2012,** 32, 410-427.
7. Mach, R. H.; Smith, C. R.; Al-Nabulsi, I.; Whirrett, B. R.; Childers, S. R.; Wheeler, K. T. $\sigma_2$ receptors as potential biomarkers of proliferation in breast cancer. *Cancer Res.* **1997,** 57, 156-161.
8. Al-Nabulsi, I.; Mach, R. H.; Wang, L. M.; Wallen, C. A.; Keng, P. C.; Sten, K.; Childers, S. R.; Wheeler, K. T. Effect of ploidy, recruitment, environmental factors, and tamoxifen treatment on the expression of sigma-2 receptors in proliferating and quiescent tumour cells. *Br. J. Cancer* **1999,** 81, 925-933.
9. Wheeler, K. T.; Wang, L. M.; Wallen, C. A.; Childers, S. R.; Cline, J. M.; Keng, P. C.; Mach, R. H. Sigma-2 receptors as a biomarker of proliferation in solid tumours. *Br. J. Cancer* **2000,** 82, 1223-1232.
10. Tu, Z.; Xu, J.; Jones, L. A.; Li, S.; Dumstorff, C.; Vangveravong, S.; Chen, D. L.; Wheeler, K. T.; Welch, M. J.; Mach, R. H. Fluorine-18-labeled benzamide analogues

for imaging the $\sigma_2$ receptor status of solid tumors with Positron Emission Tomography. *J. Med. Chem.* **2007,** 50, 3194-3204.
11. Dehdashti, F.; Laforest, R.; Gao, F.; Shoghi, K. I.; Aft, R. L.; Nussenbaum, B.; Kreisel, F. H.; Bartlett, N. L.; Cashen, A.; Wagner-Johnson, N.; Mach, R. H. Assessment of cellular proliferation in tumors by PET using $^{18}$F-ISO-1. *J. Nucl. Med.* **2013,** 54, 350-357.
12. Shoghi, K. I.; Xu, J.; Su, Y.; He, J.; Rowland, D.; Yan, Y.; Garbow, J. R.; Tu, Z.; Jones, L. A.; Higashikubo, R.; Wheeler, K. T.; Lubet, R. A.; Mach, R. H.; You, M. Quantitative receptor-based imaging of tumor proliferation with the sigma-2 ligand [$^{18}$F]ISO-1. *PLOS ONE* **2013,** 8, e74188.
13. Mach, R. H.; Wheeler, K. T. Development of molecular probes for imaging sigma-2 receptors in vitro and *in vivo*. *Cent. Nerv. Syst. Agents Med. Chem.* **2009,** 9, 230-245.
14. Sai, K. K. S.; Jones, L. A.; Mach, R. H. Development of $^{18}$F-labeled PET probes for imaging cell proliferation. *Curr. Top. Med. Chem.* **2013,** 13, 892-908.
15. Mach, R. H.; Zeng, C.; Hawkins, W. G. The $\sigma_2$ receptor: a novel protein for the imaging and treatment of cancer. *J. Med. Chem.* **2013,** 56, 7137-7160.
16. Bailey, D. L.; Willowson, K. P. An evidence-based review of quantitative SPECT imaging and potential clinical applications. *J. Nucl. Med.* **2013,** 54, 83-98.
17. John, C. S.; Lim, B. B.; Geyer, B. C.; Vilner, B. J.; Bowen, W. D. $^{99m}$Tc-labeled σ-receptor-binding complex: synthesis, characterization, and specific binding to human ductal breast carcinoma (T47D) cells. *Bioconjugate Chem.* **1997,** 8, 304-309.
18. Choi, S. R.; Yang, B.; Plössl, K.; Chumpradit, S.; Wey, S. P.; Acton, P. D.; Wheeler, K.; Mach, R. H.; Kung, H. F. Development of a Tc-99m labeled sigma-2 receptor-specific ligand as a potential breast tumor imaging agent. *Nucl. Med. Biol.* **2001,** 28, 657-666.
19. Friebe, M.; Mahmood, A.; Bolzati, C.; Drews, A.; Johannsen, B.; Eisenhut, M.; Kraemer, D.; Davison, A.; Jones, A. G. [$^{99m}$Tc]Oxotechnetium(V) complexes of amine-amide-dithiol chelates with dialkylaminoalkyl substituents as potential diagnostic probes for malignant melanoma. *J. Med. Chem.* **2001,** 44, 3132-3140.
20. Fan, C.; Jia, H.; Deuther-Conrad, W.; Brust, P.; Steinbach, J.; Liu, B. Novel $^{99m}$Tc labeled σ receptor ligand as a potential tumor imaging agent. *Sci. China Ser. B* **2006,** 49, 169-176.
21. Lu, J.; Kong, D.; Jia, H.; Deuther-Conrad, W.; Brust, P.; Wang, X. Preparation and biological evaluation of $^{99m}$TcN-4-(cyclohexylpiperazin-1-yl)dithioformate as a potential sigma receptor imaging agent. *J. Labelled Compd. Radiopharm.* **2007,** 50, 1200-1205.
22. Chen, X.; Cui, M. C.; Deuther-Conrad, W.; Tu, Y. F.; Ma, T.; Xie, Y.; Jia, B.; Li, Y.; Xie, F.; Wang, X.; Steinbach, J.; Brust, P.; Liu, B. L.; Jia, H. M. Synthesis and biological evaluation of a novel $^{99m}$Tc cyclopentadienyl tricarbonyl complex ([(Cp-R)$^{99m}$Tc(CO)$_3$]) for sigma-2 receptor tumor imaging. *Bioorg. Med. Chem. Lett.* **2012,** 22, 6352-6357.
23. Xie, F.; Kniess, T.; Neuber, C.; Deuther-Conrad, W.; Mamat, C.; Lieberman, B. P.; Liu, B.; Mach, R. H.; Brust, P.; Steinbach, J.; Pietzsch, J.; Jia, H. Novel indole-based sigma-2 receptor ligands: synthesis, structure-affinity relationship and antiproliferative activity. *Med. Chem. Comm.* **2015,** 6, 1093-1103.
24. Fan, K. H.; Lever, J. R.; Lever, S. Z. Effect of structural modification in the amine portion of substituted aminobutyl-benzamides as ligands for binding $\sigma_1$ and $\sigma_2$ receptors. *Bioorgan. Med. Chem.* **2011,** 19, 1852-1859.
25. Wang, X.; Li, D.; Deuther-Conrad, W.; Lu, J.; Xie, Y.; Jia, B.; Cui, M.; Steinbach,

J.; Brust, P.; Liu, B.; Jia, H. Novel cyclopentadienyl tricarbonyl $^{99m}$Tc complexes containing 1-piperonylpiperazine moiety: potential imaging probes for sigma-1 receptors. *J. Med. Chem.* **2014,** 57, 7113-7125.
26. Shumway, S. D.; Toniatti, C.; Roberts, B. S.; Martin, M. M. Compositions and methods for treating cancer. WO2013039854A1, 2013.
27. Mach, R. H.; Huang, Y.; Freeman, R. A.; Wu, L.; Vangveravong, S.; Luedtke, R. R. Conformationally-flexible benzamide analogues as dopamine $D_3$ and $\sigma_2$ receptor ligands. *Bioorg. Med. Chem. Lett.* **2004,** 14, 195-202.
28. Peindy N'Dongo, H. W.; Liu, Y.; Can, D.; Schmutz, P.; Spingler, B.; Alberto, R. Aqueous syntheses of [(Cp-R)M$(CO)_3$] type complexes (Cp = cyclopentadienyl, M = Mn, $^{99m}$Tc, Re) with bioactive functionalities. *J. Organomet. Chem.* **2009,** 694, 981-987.
29. Li, D.; Wang, X.; Deuther-Conrad, W.; Chen, X.; Cui, M. C.; Steinbach, J.; Brust, P.; Liu, B.; Jia, H. Synthesis and preliminary evaluation of novel [(Cp-R)M$(CO)_3$] (M = Re, $^{99m}$Tc) complexes as potent sigma-2 receptor ligands. *J. Labelled. Compd. Rad.* **2013**, 56, S383.
30. Chen, Y.; Deuther-Conrad, W.; Steinbach, J.; Brust, P.; Liu, B.; Jia, H. A novel cyclopentadienyl tricarbonyl $^{99m}$Tc complex containing 5,6-dimethoxyisoindoline motif – synthesis and evaluation of a radiotracer for imaging of sigma-2 receptors in cancer. *J. Labelled. Compd. Rad.* **2015**, 58, S98.
31. Perregaard, J.; Moltzen, E. K.; Meier, E.; Sanchez, C. Sigma ligands with subnanomolar affinity and preference for the sigma 2 binding site. 1. 3-(omega-aminoalkyl)-1H-indoles. *J. Med. Chem.* **1995,** 38, 1998-2008.
32. Niso, M.; Abate, C.; Contino, M.; Ferorelli, S.; Azzariti, A.; Perrone, R.; Colabufo, N. A.; Berardi, F. Sigma-2 receptor agonists as possible antitumor agents in resistant tumors: hints for collateral sensitivity. *Chem. Med. Chem.* **2013,** 8, 2026-2035.
33. Wang, X.; Li, Y.; Deuther-Conrad, W.; Xie, F.; Chen, X.; Cui, M.-C.; Zhang, X.-J.; Zhang, J.-M.; Steinbach, J.; Brust, P.; Liu, B.-L.; Jia, H.-M. Synthesis and biological evaluation of $^{18}$F labeled fluoro-oligo-ethoxylated 4-benzylpiperazine derivatives for sigma-1 receptor imaging. *Bioorgan. Med. Chem.* **2013,** 21, 215-222.
34. Laruelle, M.; Slifstein, M.; Huang, Y. Relationships between radiotracer properties and image quality in molecular imaging of the brain with positron emission tomography. *Mol. Imaging Biol.* **2003**, 5, 363-75.
35. Huang, Y.; Zheng, M.-Q.; Gerdes, J. M. Development of effective PET and SPECT imaging agents for the serotonin transporter: has a twenty-year journey reached its destination? *Curr. Top. Med. Chem.* **2010**, 10, 1499-1526.
36. Li, Y.; Wang, X.; Zhang, J.; Deuther-Conrad, W.; Xie, F.; Zhang, X.; Liu, J.; Qiao, J.; Cui, M.; Steinbach, J.; Brust, P.; Liu, B.; Jia, H. Synthesis and evaluation of novel $^{18}$F-labeled spirocyclic piperidine derivatives as $\sigma_1$ receptor ligands for positron emission tomography imaging. *J. Med. Chem.* **2013,** 56, 3478-3491.
37. Glennon, R. A. Binding characteristics of $\sigma_2$ receptor ligands. *Rev. Bras. Cienc. Farm.* **2005,** 41, 1-12.
38. Sorger, D.; Scheunemann, M.; Grossmann, U.; Fischer, S.; Vercouille, J.; Hiller, A.; Wenzel, B.; Roghani, A.; Schliebs, R.; Brust, P.; Sabri, O.; Steinbach, J. A new $^{18}$F-labeled fluoroacetylmorpholino derivative of vesamicol for neuroimaging of the vesicular acetylcholine transporter. *Nucl. Med. Biol.* **2008**, *35*, 185-195.
39. Saidi, M.; Kothari, K.; Pillai, M. R. A.; Hassan, A.; Sarma, H. D.; Chaudhari, P. R.; Unnikrishnan, T. P.; Korde, A.; Azzouz, Z. Cyclopentadienyl technetium ($^{99m}$Tc) tricarbonyl piperidine conjugates: biodistribution and imaging studies. *J. Labelled.*

*Compd. Rad.* **2001,** 44, 603-618.